TLR3 Deficiency Leads to Altered Immune Responses to *Chlamydia trachomatis* Infection in Human Oviduct Epithelial Cells

Jerry Z. Xu[1¶], Ramesh Kumar[1¶], Haoli Gong[2], Luyao Liu[2], Nicole Ramos-Solis[1], Yujing Li[3], and Wilbert A. Derbigny[1*]

[1]Department of Microbiology and Immunology; Indiana University School of Medicine, Indianapolis, Indiana, United States of America.

[3]Department of Medical and Molecular Genetics, Indiana University School of Medicine, Indianapolis, Indiana, United States of America.

[2]Xiangya Second Hospital, Central South University, Peoples Republic of China.

[¶]These authors contributed equally to this work.

*Corresponding author:

Email: wderbign@iupui.edu

Running Title: TLR3 deficiency in human *Chlamydia* infection

ABSTRACT

Reproductive tract pathology caused by *Chlamydia trachomatis* infection is an important global cause of human infertility. To better understand the mechanisms associated with *Chlamydia*-induced genital tract pathogenesis in humans, we used CRISPR genome editing to disrupt TLR3 function in the human oviduct epithelial (hOE) cell-line OE-E6/E7, in order to investigate the possible role(s) of TLR3 signaling in the immune response to *Chlamydia*. Disruption of TLR3 function in these cells significantly diminished the *Chlamydia*-induced synthesis of several inflammation biomarkers including IFN-β, IL-6, IL-6Ra, sIL-6Rβ (gp130), IL-8, IL-20, IL-26, IL-34, sTNF-R1, TNFSF13B, MMP-1, MMP-2, and MMP-3. In contrast, the *Chlamydia*-induced synthesis of CCL-5, IL-29 (IFNλ1) and IL-28A (IFNλ2) were significantly *increased* in the TLR3-deficient hOE cells when compared to their wild-type counterparts. Our results propose a role for TLR3 signaling in limiting the genital tract fibrosis, scarring, and chronic inflammation often associated with human chlamydial disease. Interestingly, we saw that *Chlamydia* infection induced the production of biomarkers associated with persistence, tumor metastasis, and autoimmunity such as soluble CD163 (sCD163), chitinase-3-like protein 1, osteopontin, and pentraxin-3 in the hOE cells; however, their expression levels were significantly dysregulated in the TLR3-deficient hOE cells. Finally, we demonstrate using the hOE cells that TLR3 deficiency resulted in an increased amount of chlamydial LPS within the *Chlamydia* inclusion, which is suggestive that TLR3 deficiency leads to enhanced chlamydial replication and possibly increased genital tract pathogenesis during human infection.

KEYWORDS: *Chlamydia trachomatis*, TLR3, human oviduct epithelial cells.

Abbreviations: hOE, human OE-E6/E7 cells; TLR3 KO, TLR3 knockout cell line; poly (I:C), Polyinosinic–polycytidylic acid sodium salt.

Introduction

The bacterial pathogen *Chlamydia trachomatis* has caused 1,526,658 infections in the United States in 2015 (an increase of 6% since 2014), and it is the most commonly reported bacterial sexually transmitted disease (STD) in the United States (1). Genital tract *C. trachomatis* infections are easily cured with antibiotics if properly diagnosed at early stages of infection. However, because 75-90% of women infected with *Chlamydia* are asymptomatic for clinical disease, opportunities for therapeutic interventions are usually missed. The asymptomatic nature of the clinical symptoms is the major contributing factor to the continuing spread of the disease to uninfected partners, and the more severe pathogenesis and sequelae that often lead to infertility in women. Further contributing to the growing rates of infectivity amongst the previously uninfected populations are the statistics showing that up to 90% of men infected with *Chlamydia* exhibit no symptoms (2, 3) and that an effective vaccine remains elusive (4).

Chlamydia infections are also leading causes of pelvic inflammatory disease (5), tubal occlusion (6), and ectopic pregnancy (7, 8) in women. Interactions between the host immunity and *Chlamydia* infection are thought to be largely responsible for the pathology associated with human chlamydial disease, though the precise pathogenic mechanisms remain unclear (9, 10). As an obligate intracellular pathogen, *Chlamydia* species are known to interact with host-cell pattern recognition receptors (PRRs), including a variety of intracellular cytosolic receptors and Toll-like receptors (TLRs), to trigger the innate-immune inflammatory response (11-18). Stimulation of genital tract epithelial cell TLRs (and other PRRs) by chlamydial pathogen-associated molecular patterns (PAMPs) trigger cytokine responses that are critical to the establishment of

innate and adaptive immunity. These *Chlamydia*-induced cytokine responses also include the syntheses of inflammatory mediators that have been implicated as the major culprit in the pathology associated with *Chlamydia* disease (12, 14, 19-24). The overall goal of these investigations into the interactions between host-cell PRRs and *Chlamydia* infection is to identify the PRRs that trigger specific inflammatory mediators that cause scarring and fibrosis, and then define therapeutic measures to prevent that process.

Human genital tract epithelial cells express most of the known TLRs; however, the TLRs are known to vary in their expression levels within the female reproductive tract (depending upon the concentration of specific sex hormones) and their tissue distribution (25). The human Fallopian-derived epithelial cell line OE-E6/E7 (26) was shown to express functional proteins for TLRs 1 through 6, of which TLR2 was shown to have a role in the innate-immune response to *C. trachomatis* infection (27, 28). TLR2 has also been shown to have a role in the immune responses to *C. muridarum* infection in mice, and that it had a significant role in the *Chlamydia*-induced genital tract pathology observed in the infected animals (12, 29-31). In our early investigations into the role of TLR3 in the immune response to genital tract *Chlamydia* infection, we showed that *C. muridarum* infected murine oviduct epithelial (OE) cells secrete IFN-β in a mostly TLR3 dependent manner, and that mouse OE cells deficient in TLR3 show dramatic reductions in the synthesis of other inflammatory immune mediators in addition to IFN-β (13, 15). Our most recent report shows that TLR3-deficient mice have increased chlamydial loads, aberrant genital tract secretion levels of several different inflammatory mediators, an altered $CD4^+$ T-cell recruitment, and more severe oviduct and uterine horn pathology when compared to wild-type controls (32). Our data propose

a protective role for TLR3 signaling in the immune response to *Chlamydia* infection in mice. However, the role of TLR3 in the immune response to *Chlamydia* infection in human oviduct tissue has not yet been investigated and remains unclear. In this study, we used the immortalized human oviduct epithelial cell line OE-E6/E7 to assess the role of TLR3 in the immune responses to *Chlamydia trachomatis* L2 infection.

MATERIALS AND METHODS

Cell culture

Human OE-E6/E7 (hOE) cells and Hela cells were maintained in high glucose Dulbecco's modified Eagle's medium (Life Technologies, Inc.) supplemented with 10% bovine calf serum (Hyclone) in a 37 °C, 5% CO_2 incubator. The hOE cells were originally derived from Fallopian tube tissue and were immortalized by expressing the HPV 16 E6/E7 open reading frame in a retroviral expression system (26).

Reagents

The following TLR agonists were purchased from InVivoGen (San Diego, CA): 1) peptidoglycan from *E. coli* serotype 0111:B4 (125 EU/mg); 2) ultrapure flagellin purified from isolated from *Bacillus subtilis* (>95% purity); and 3) ODN 2216, a synthetic oligonucleotide (ODN) that preferentially binds human TLR9 and ODN2243, an ODN 2216 control without CpGs. Wildtype (WT) and TLR3-deficient hOE cells were grown to confluence in 24-well before being treated with the appropriate TLR ligand at the

concentrations specified in the text. Supernatants were harvested at the 24h post-treatment time point and analyzed for cytokine content using ELISA for IL-6 (R&D Systems; Minneapolis, MN) according to the manufacturer's protocol

Generating theTLR3-deficient human epithelial cell lines

The human OE-E6/E7 cells and Hela cells were grown to 60-70% confluence before being transduced with either the human TLR3 CRISPR knockout Lentivirus or the CRISPR-Lenti non-targeting control transduction particles and 4µg/µL Polybrene. The Lenti-CRISPR Transduction particles (pLV-U6g-EPCG-TLR3), All-in-one ready-to-use Cas9 and guide RNA (gRNA), and CRISPR negative controls were purchased from Sigma (Sigma-Aldrich; St Louis, MO). The CRISPR system consisted of 3 gRNA sequences (CCACCTGAAGTTGACTCAGGTA, CCAACTTCACAAGGTATAGCCA, and CAGGGTGTTTTCACGCAATTGG), which targeted the human TLR3 gene (NM_003265) at exon 2, exon 2, and exon 4 respectively. The CRISPR Universal negative control targets no known human, mouse, or rat gene. The transduced human OE-E6/E7 cells and Hela cells were subjected to 5µg/mL puromycin selection, and the puromycin-resistant cells were sorted by using BD FACSAria cell sorter. The brightest GFP positive cells were collected and cultured for further single-cell cloning by glass cloning cylinders. Individual cell colonies were isolated and expanded. Higher GFP expressing cell clones were further selected by using BD Accuri C6 flow cytometer. Confirmation of TLR3 gene deletion, protein expression, and receptor function was assessed using PCR, western blot, and ELISA, respectively.

Genomic DNA purification and PCR-amplification

Genomic DNA (gDNA) from hOE-TLRKO was purified by using the PureLink Genomic DNA Mini Kit from Invitrogen (Invitrogen Catlog# K1820-01). The gene-specific primer pairs (forward 5'-ACA AGG AAT ATA CCA ATG CAT TTG-3'and reverse 5'-GAT ATT TAG ATA GTA AGT CTA AGG-3') were designed approximate 300 bps Up-and Down streams of the gRNA (CCACCTGAAGTTGACTCAGGTA) sequence spanning exon-2 of TLR3 gene. The purified g-DNA as a template and Platinum Super-Fi PCR master mix (Invitrogen Catlog# 12358-010) were used to amplify the PCR product (599bps). The cycling conditions were as: initial denaturation at 95°C for 2 min followed by 32 cycles, denaturation at 95°C for 45 s, annealing at 50.5°C for 45 s, elongation at 72°C for 45 s and final elongation at 72°C for 2 min. The amplified PCR products were gel purified using the QIAquick gel extraction kit (Qiagen; Germantown, MD). The PCR product from hOE-WT cells was used as control sample throughout this experiment. A portion of the amplified PCR products was sent for sequencing at the IUSM Bioinformatics Core Sequencing Facility, while the rest of the PCR products were used in the cloning experiment.

Cloning and Plasmid Purification

An additional adenine-overhang was added to the portion of the PCR product to be cloned by using hi-fidelity Taq-polymerase and dATP at 70°C for 20min. The reaction mixtures were then ligated into pGEM-T Easy vector (Promega Catlog#A1360)

overnight at 4°C and then transformed into TOP10 competent *E. coli*. The transformed *E. coli* were plated on LB-agar plates containing ampicillin (60ug/ml) supplemented with IPTG. The blue and white colonies were screened and inoculated into 5ml LB medium containing Amp (final concentration 60ug/ml). The putative positive cultures were used for plasmid purification by using QiaSpin Miniprep Kit (Catlog# 27106), and inserts were confirmed by PCR before plasmid sequencing.

Chlamydia trachomatis **preparation**

The *C. trachomatis* L2-434/Bu (L2) and *C. trachomatis* UW-3CX serovar D strains were generously provided by Dr. David E. Nelson. The *C. trachomatis*-serovar D and L2 mother pools used in these experiments were subsequently grown and titrated as described in (33), whereby antibody specific for chlamydial LPS was used to identify chlamydial inclusions in the infected Hela cells. Alexa Fluor 488 and Alexa Fluor 594 anti-mouse IgG antibodies used in these experiments were purchased from Invitrogen (Invitrogen/Life Technologies; Carlsbad, CA), and immuno-staining results for titration of infectious chlamydial elementary bodies (EBs) were scanned and recorded by EVOS FL auto cell imaging system (Thermo-Fisher, Pittsburgh, PA). The corresponding isotype controls were used as negative controls.

hOE and Hela cell Infections

OE-E6/E7 and Hela cells were plated in either 12 or 6-well tissue culture plates and grown to 80-90% confluence. For all experiments (unless stated otherwise), the cells

were infected with 10 inclusion-forming-units (IFU) of *C. trachomatis*/ cell in cell culture medium. Immediately after adding *Chlamydia*, the tissue culture plates were gently agitated, centrifuged at 1200 rpm (200 × g) in a table-top centrifuge for 1 hour, and then incubated at 37°C in a 5% CO_2 humidified incubator without subsequent change of medium until the time of cell harvest. Mock-infected control cells received an equivalent volume of epithelial cell culture medium but lacked any viable *C. trachomatis*.

Protein extraction and evaluating protein expression levels

Epithelial cell lysates were prepared via incubation of PBS washed cell monolayers in RIPA buffer (EMD Millipore; Burlington, Massachusetts) with the addition of 1mM PMSF and 1x Protease Inhibitor Cocktails (Sigma). The total protein concentration of each sample was determined by using the Pierce BCA protein assay (Thermo Scientific). Analyses of protein expression were performed by using the WES™ simple western system (ProteinSimple; San Jose, California). Endogenous TLR3 protein expression in the wild type (WT) and CRISPR-modified epithelial cells was detected using a 1:50 dilution of TLR3 monoclonal antibody (Abcam; Cambridge, MA). Relative TLR3 protein expression levels between WT and CRISPR modified cells were obtained by measuring TLR3's expression against the intracellular β-Actin control protein bound to an anti-β-Actin monoclonal antibody (1:300; Sigma). Protein detection in WES was accomplished according to the manufacturer's protocol using streptavidin-HRP based methodology (ProteinSimple). The positive control for testing antibody specificity for TLR3 expression included loading (in separate reactions) either 50ng or 100ng of HEK293 cell lysate overexpressing human TLR3 (Novus).

209

210 **RNA purification and real-time quantitative PCR (RT-qPCR)**

211 Total cell RNA was isolated from mock and *C. trachomatis*-infected WT and TLR3-
212 deficient epithelial cells using the RNeasy kit plus (Qiagen, Valencia, CA). The DNA-
213 free RNA was quantified using the NanoDrop spectrophotometer (Thermo Scientific),
214 and cDNA was obtained with the Applied Biosystem's high-capacity cDNA reverse
215 transcription kit (Thermo Fisher). Target mRNA was quantified using Applied
216 Biosystem's TaqMan gene-expression master kit in reactions containing either human
217 TLR3 primers, human IFN-β primers, and/or β-actin control primers. Quantitative
218 measurements were performed via the ABI7500 real-time PCR detection system
219 (Thermo Fisher).

220

221 **Standard and Multiplex ELISA analyses**

222 The human IFN-β ELISA Kit (cat. #41410-1) and IL-6 ELISA kit (cat. #D6050)
223 purchased from R&D systems were used to measure the *Chlamydia*-induced IFN-β and
224 IL-6 respectively, using the manufacturer's protocol. The standard ELISA kits were
225 used to measure single cytokines secreted into the supernatants of hOE-WT, hOE- N-
226 Ctrl, and hOE-TLRKO- cells that were either mock treated, infected with *C. trachomatis*,
227 or treated with various TLR agonist.

228 To measure the chlamydial induced syntheses of several immune factors
229 simultaneously, WT and TLR3 deficient hOE cells were either mock treated or infected
230 at a MOI of 10 IFU/ cell with either serovar D or the L2 strain of *C. trachomatis*. For *C.*

231 *trachomatis*-L2 infections, the supernatants were harvested at 0 (mock), 6, 12, 18, 24,
232 and 30hrs post infection. The supernatants from the L2 infections were subjected to
233 multiplex ELISA analyses in triplicate setting using the Bio-Plex Pro human
234 inflammation panel-1, 37-Plex #171AL001M (Bio-Rad; Hercules, California) according
235 to the manufacturer's instructions. For infections with *C. trachomatis*-serovar D, the
236 supernatants were harvested at 0 (mock), 6, 12, 24, 36, 48, 60, and 72hrs post
237 infection. The supernatants from the serovar D infections were subjected to multiplex
238 ELISA analyses in triplicate setting using a custom designed 27-plex human magnetic
239 Luminex assay #LXSAHM (R&D Systems) according to the manufacturer's instructions.
240 Analyses of the data were performed in concert with the Indiana University Multiplex
241 Analysis Core located in the Melvin and Bren Simon Cancer Center.

242

243 **RNA-interference**

244 The transfections of the TLR3-specific siRNA (cat. #AM16708; Ambion/ Thermo-Fisher)
245 and the scrambled control RNA (Silencer™ negative control; Thermo-Fisher) were done
246 using Lipofectamine RNAiMAX (Thermo-Fisher) as described in (34). Briefly, 75-80%
247 confluent hOE-WT cells were transfected with 2.5ug of each siRNA for 24 hours at 37°C
248 with 5% CO2. After the 24h period, cell supernatants were replaced with fresh media
249 prior to being infected with 10 IFU/cell *C. trachomatis*-L2. The level of IFN-β expression
250 was determined at the specified time post infection by ELISA as described above.

251

252 **Flow cytometric analysis and multi-spectral imaging flow cytometry**

WT and TLR3 deficient epithelial cells were either mock treated or infected at a MOI of 10 IFU/ cell with *Chlamydia trachomatis* L2 for 24 hours. At the 24hr time point, monolayers were washed once with PBS/2mM EDTA before being gently removed from the plate with trypsin-versene, washed 3 times in ice-cold PBS/EDTA, and cell pellets resuspended in 4% Formalin for 30 min at room temperature. The cells were washed 3 times with PBS/ EDTA and were permeabilized in 0.3% Triton X-100/ PBS/EDTA for 5 min at room temperature. The cells were blocked in blocking buffer (5% FBS/0.1%BSA/0.1%Triton X-100/PBS/EDTA) at room temperature for 60min. The cells were stained with anti-chlamydia LPS antibody (from Dr. David E. Nelson) in blocking buffer (1:5) for 60 min at room temperature. The cells were washed 3 times with PBS/EDTA. The cells were further stained with secondary antibody APC anti-mouse IgG(H+L) (1:1000, ThermoFisher) in blocking buffer for 30min before being washed 3 times with PBS/EDTA. Finally, the cells were suspended in 0.6ml 2% FBS/PBS/EDTA for flow cytometry analysis. Cellular responses to *Chlamydia* infection were analyzed via BD LSRFortessa cell analyzer (Becton Dickinson; Franklin Lakes, NJ) or by Multi-spectral Imaging Flow Cytometer Amnis Image StreamX MKII (EMD Millipore). Data were interpreted by using FlowJo v10 (FlowJo, LLC) and IDEAS (EMD Millipore) software.

Immunofluorescent Staining

WT and TLR3 deficient hOE cells were seeded in 96-well μ-plate (Ibidi; Fitchburg, WI) and allowed to grow to 90% confluence before being either mock treated or infected at a MOI of 5 IFU/ cell with *C. trachomatis*-serovar D. At 36 hours post infection, the

infected cells were then fixed with 200 µl of methanol and incubate at room temperature for 10 minutes. The fixed cells were stained with a 1:100 dilution of anti-chlamydial LPS antibody (EVI-HI; provided to us by Dr. David E. Nelson) and incubated for 1 hour at room temperature. The stained cells were washed 3 times with PBS. Detection was accomplished with a secondary stain of Alexa Fluor 488 and Alexa Fluor 594 anti-mouse IgG antibodies (Invitrogen). Nuclei were counterstained with 4,6-diamidino-2-phenylindole (DAPI; Life Technologies) according to manufacturer's protocol and imaged at 60X under oil immersion using a Nikon Eclipse Ti microscope.

Statistical Analysis

Numerical data are presented as means ± SEM. All experiments were repeated at least three times, and statistical significance was determined using either 2-way *ANOVA* analyses in GraphPad Prism or Student's two-tailed *t*-test. Statistically significant differences are shown by asterisks (*) and with the minimum criteria being $p < 0.05$.

RESULTS

IFN-β is induced in human OE-E6/7 cells in response to *Chlamydia* infection

IFN-β is known to be expressed during activation of the TLR3 signaling pathway during certain viral infections, and by stimulation via the synthetic double-stranded RNA analog poly (I:C) (35, 36). To confirm the presence of TLR3 and ascertain its function in the human OE-E6/E7 cells (hOE), the hOE cells were incubated in cell culture media

297 supplemented with increasing concentrations of poly (I:C) for 24hrs. Figure 1A shows
298 that the relative IFN-β mRNA expression was increased at the concentrations of 25, 50,
299 and 100 µg/mL when compared to untreated controls. These results confirm that the
300 TLR3 is functional in the hOE cells by demonstrating a dose-dependent increase in IFN-
301 β gene expression in response to poly (I:C) stimulation. To ascertain the impact of
302 *Chlamydia* infection on IFN-β synthesis in the hOE cells, we next infected hOE cells
303 with *Chlamydia trachomatis* L2 at a MOI of 10 IFU/ cell for 24hrs, and measured the
304 mRNA expression levels of both IFN-β and TLR3. As shown in Figures 1B and 1C,
305 mRNA expression levels of IFN-β and TLR3 were increased during *Chlamydia* infection.
306 These data are suggestive that *Chlamydia* infection of the hOE cells induces IFN-β
307 synthesis and upregulates TLR3 gene expression in human oviduct tissue in a similar
308 manner to what we have observed in the murine oviduct epithelial cells (14, 24). These
309 findings provide the impetus for us to extrapolate that the IFN-β induced during
310 *Chlamydia* infection in hOE cells will also occur via TLR3-dependent mechanisms
311 similar to what we have reported in the murine OE cells (13).

312

313 **Disruption of TLR3 function in human genital tract epithelial cells and clone**
314 **identification**

315 To ascertain the role of TLR3 in the innate-immune response to human genital tract
316 *Chlamydia* infections *in vitro*, we disrupted TLR3 function in both human oviduct (hOE
317 cells) and cervical (Hela cells) tissue using the Sigma CRISPR Lentivirus system (see
318 Materials and Methods). The CRISPR system consisted of 3 gRNA sequences which
319 targeted human TLR3 gene at exon 2, exon 2, and exon 4 respectively (Fig. S1). To

ascertain the efficacy of using this approach to disrupt TLR3 function in these cells, we first examined the TLR3 protein expression levels in the putative clones by using capillary electrophoresis in the Wes™ system to identify and quantitate TLR3 protein. In these experiments, we loaded a total 400ng of cell lysate isolated from each of the selected clones and the WT control cells. Figure 2 shows the results of capillary electrophoresis in which we simultaneously immunoassayed for both TLR3 expression and the β-Actin loading control in hOE cells, Hela cells, and the representative TLR3-deficient clones generated in each parental cell-line. As shown, a major band indicative of the TLR3 protein expression was identified in the hOE and Hela cells, with a peak molecular weight of 174kDa and 187kDa, respectively. Our data are suggestive that the TLR3 protein is post-translationally modified in different ways in the different cell types, which affects their electrophoretic migration and apparent molecular weight (37).

A qualitative examination of Figure 2 shows that TLR3 protein expression levels were substantially lower in both clone #8 of the hOE-TLR3KO cells and clone #16 of the Hela TLR3KO cells when compared to their wild-type counterparts. These clones were selected and used as TLR3-deficient versions of the human OE-E6/7 cells and the Hela cells, respectively, and were quantitatively analyzed for actual TLR3 expression levels in the Wes™ Compass software. To ascertain the actual level of reduction in TLR3 protein expression levels, the protein band peaks were identified and quantified using the chemiluminescence peak area of the Wes™ generated data. The ratio of TLR3 protein expression compared to that of the β-Actin loading control was used as the index for calculating relative TLR3 protein expression level. In the hOE cells, the ratios of TLR3/β-Actin for WT and TLR3KO were 5732/41538=0.138 and 347/16533=0.021,

respectively. When calculated, the TLR3 protein expression was down about 85% in clone #8 of the hOE-TLR3KO cells. In Hela cells, the ratio of TLR3/β-Actin for WT and TLR3KO was 9254/43601=0.212 and 310/16482=0.018, respectively. The calculated expression level of TLR3 protein was down about 94% in clone #16 of the Hela TLR3KO cells. Collectively, our findings demonstrate that CRISPR Lentivirus system was very effective in disrupting TLR3 protein expression in both of these cell types.

TLR3 deficiency in human genital tract epithelial cells results in a decreased IFN-β synthesis in response to poly (I:C) stimulation and chlamydial infection.

To determine whether the TLR3-deficient clones representing human oviduct and cervical tissue were also deficient in their ability to elicit appropriate TLR3-dependent innate-immune responses, we first treated the clone representative of each cell type with 0, 25, 50, 100 µg/mL the TLR3 agonist poly (I:C) for 24hrs and assessed TLR3's functionality by measuring the induction of IFN-β gene expression (Figure 3). As shown in Figure 3A, the hOE TLR3KO cells exhibited significantly lower levels of IFN-β gene expression in response to poly (I:C) induction at all concentrations tested when compared to the non-target CRISPR control cells. We observed similar reductions in the induction of IFN-β transcription in response to poly (I:C) in the representative Hela TLR3KO clones (Figure 3B). However, the fold-difference in IFN-β gene induction between the TLR3-deficient clones and the non-target CRISPR control for the Hela cells seemed to decrease at the higher poly (I:C) concentrations. We observed no noticeable differences in poly (I:C) induction of IFN-β transcription between the WT cells and their non-target CRISPR control counterpart for either cell type *(data not shown).* These

findings show a successful disruption of TLR3 function in the TLR3-deficient epithelial cell clones representing human oviduct and cervical tissues.

In order to make comparisons to what we have previously reported on the role of TLR3 in the innate immune response to *Chlamydia* infection in the murine oviduct epithelial cells, we put more emphasis on the hOE cells in this study and selected the hOE TLR3KO clone #8 for use in the remainder of this report. We first sought to ascertain the impact of TLR3 deficiency on the *C. trachomatis*-induced synthesis of IFN-β in the human oviduct epithelial cells. We infected hOE-WT, hOE N-Ctrl, and hOE-TLR3KO cells with 10 IFU *C. trachomatis*-L2 before harvesting cell supernatants at 18 and 36h post-infection to measure the amount of IFN-β secreted. Figure 4A shows a significant reduction in the *Chlamydia*-induced synthesis of IFN-β in the TLR3-deficient hOE cells when compared to both the WT and non-template control cells. Our data show a 40-50% reduction in the amount of IFN-β synthesized at both time-points and are suggestive that TLR3 plays a significant role in the optimal synthesis of IFN-β in *C. trachomatis* infected hOE cells.

We next assessed whether our limiting dilution clonal expansion procedure introduced 'founder effects' such as causing a global dysregulation in TLR signaling that leads to the diminished synthesis of inflammatory cytokines during *Chlamydia* infection in hOE TLR3KO cells. To test whether there were founder effects introduced that negatively impacted TLR signaling in a global manner, we treated WT and TLR3-deficient hOE cells with ultrapure preparations of ligands for TLR2 (peptidoglycan), TLR5 (flagellin), and TLR9 (ODN-CpG) for 24hrs before testing supernatants for IL-6 synthesis by ELISA (14). As shown in Fig. S2, we saw no significant differences

between WT and TLR3-deficient hOE cells in the synthesis of IL-6 when the cells were treated with agonists for either TLR2, TLR5, or TLR9. To address the possibility that reduced IFN-β synthesis observed in the hOE-TLR3KO cells was due to pathways unrelated to TLR3 that may have been disrupted by CRISPR, we used siRNA as an alternative method to transiently disrupt TLR3 gene expression and protein function in WT hOE cells. Figure 4B demonstrates significant reductions in the amount of IFN-β secreted into the supernatants of *C. trachomatis*-L2 infected hOE cells that were pretreated with TLR3-specific siRNA 24hrs prior to infection.

To discern the exact nature of the TLR3 gene defect introduced by CRISPR-Cas9, clone #8 of the hOE-TLR3KO cells was selected for gene sequencing and gene sequence alignment in CLUSTAL-O. Analysis of the TLR3 gene sequencing data revealed that clone #8 of the hOE-TLR3KO cells was heterozygous for TLR3 gene disruption at exon #2 and that the resultant knockout allele incorporated a premature stop codon (TGA) at nucleotide position 141 (Figure 4C). The CRISPR-Cas9 method of gene disruption resulted in the translation of truncated TLR3 protein that is likely non-functional, and our collective data examining TLR3 protein expression and function (Figs 2-4 and Fig. S2) are suggestive that there is a minimal contribution from the TLR3 allele that was not disrupted by CRISPR-Cas9 at Exon #2. Collectively, these findings show that CRISPR-Cas9 methodology was effective in disrupting TLR3 gene function in hOE cells, and corroborate our previous reports that implicate TLR3 as a major contributor to the *Chlamydia*-induced synthesis of IFN-β during *Chlamydia* infection of oviduct epithelial cells (13, 38).

412 **TLR3 deficiency alters the *Chlamydia*-induced syntheses of acute inflammatory**
413 **biomarkers in human oviduct epithelial cells.**

414 We previously reported that murine OE cells showed dysregulation in the *C. muridarum*
415 induced syntheses of a multitude of acute inflammatory mediators, and subsequently
416 showed that TLR3 deficient mice exhibited increased chlamydial shedding, aberrant T-
417 cell recruitment, and more severe genital tract pathology when compared to WT mice
418 (15, 32). To assess whether the absence of TLR3 is associated with the chlamydial-
419 induced syntheses of key biomarkers of inflammation in human oviduct epithelial cells,
420 we performed multiplex ELISA analysis for the detection and quantification of key
421 human innate-immune inflammatory biomarkers. hOE-WT and hOE-TLR3KO cells were
422 either mock-infected, infected with *C. trachomatis*-L2 for up to 30hrs, or infected with *C.*
423 *trachomatis*-serovar D for up to 72hrs before multiplex analyses of the cell
424 supernatants. As shown in Figures 5 and 6, TLR3-deficient hOE cells secreted
425 significantly reduced levels of the acute inflammatory markers IL-6, IL-6Ra, sIL-6Rβ
426 (gp130), IL-8, IL-20, IL-26, and IL-34 secreted into the supernatants of the *C.*
427 *trachomatis* infected cells throughout infection. Conversely, TLR3 deficiency in hOE
428 cells resulted in the *increased* synthesis of CCL5 and the type III interferon IL-29
429 (IFNλ1) throughout infection, and IL-28A (IFNλ2) late in infection (Figures 6 and 7).
430 Collectively, these data demonstrate a putative role for TLR3 in the acute phase of the
431 innate immune response to *Chlamydia* that is known to occur early during infection *in*
432 *vivo (17, 39-42),* and that TLR3 has some role in modulating mediators of the adaptive
433 immune response (43).

434

TLR3 has a functional role in the *C. trachomatis* induced syntheses of factors associated with genital tract fibrosis, scarring, and chronic inflammation.

In our previous investigations into the role of TLR3 in the pathogenesis of genital infections in mice, one key aspect of TLR3 deficiency that we observed was that mice deficient in TLR3 appeared exhibit indicators of more pronounced chronic sequelae, such as lymphocytic endometritis and hydrosalpinx (32). To examine whether TLR3 has a similar role in the pathogenesis of genital tract *Chlamydia* infections in humans, we next measured the *Chlamydia*-induced synthesis of biomarkers associated with chronic inflammatory disease and tissue necrosis in the WT and TLR3 deficient hOE cells. As shown in Figures 8A and 8D, *C. trachomatis* infection induces the synthesis of soluble tumor necrosis factor receptor 1 (sTNF-R1) in both cell types; however, its synthesis was significantly lower in the TLR3-deficient hOE cells at mid-to-late times during infection. The exact role of sTNF-R1 in *Chlamydia* infection is not clear, but it is a known negative regulator of TNFα, which is a cytokine associated with severe genital tract sequelae in mice (44). Figure 8B shows that TLR3 deficiency leads to a similar impact on the chlamydial induced synthesis of tumor necrosis factor ligand superfamily member 13B (TNFSF13B), a cytokine that belongs to the tumor necrosis factor family that acts as a potent B-cell activator (45). Interestingly, Figures 8C and 8E shows that the syntheses of TGF-β1 and ICAM-1 is increased during *C. trachomatis* infection of hOE-TLR3KO cells, implicating TLR3 in the negative regulation of key components of the pathophysiological process of fibrogenesis (46).

The matrix metalloproteinases (MMPs) are a tightly regulated family of proteins that are involved in the breakdown of extracellular matrix in normal physiological

processes and are known to have a regulatory role in the inflammatory immune response, wound healing, cell migration, and embryonic development (47). Dysregulation of these proteins during *Chlamydia* infection has been demonstrated to play a role in the pathogenesis of fallopian tube damage during genital tract infections, and in corneal scarring in patients with trachoma (48, 49). To ascertain whether MMPs are synthesized in response to *C. trachomatis* infection in the hOE cells, and to determine whether TLR3 deficiency impacts their protein expression levels, we next measured the secretion of candidate MMPs into the supernatants of *C. trachomatis* infected cells in our multiplex ELISA. As shown in Figure 9, *Chlamydia* infection induced the production of MMP-1, MMP-2, MMP-3, and MMP-10 throughout infection, supporting the observations of others regarding the induction of MMPs in genital tract infections (48, 50-52). The *Chlamydia*-induced syntheses of these MMPs were either completely absent or severely diminished in their production in the TLR3-deficient hOE cells relative to hOE-WT cells when infected with the L2 serovar (Figures 8A-8C). However, the synthesis levels were more similar when infected with serovar D, albeit at significantly lower amounts in the hOE-TLR3KO cells at various points post-infection (Figures 8D-8F). Taken together, data from Figures 8 and 9 are suggestive that TLR3 plays some role in regulating the syntheses of immune factors involved in modulating the genital tract pathologies associated with *Chlamydia* infection in humans.

TLR3 signaling regulates the *Chlamydia*-induced synthesis of biomarkers associated with persistence, metastasis, and autoimmunity.

A major factor in the protective immune response to *C. trachomatis* infection is the synthesis of gamma-interferon (IFNγ), which inhibits the growth of chlamydial RBs via mechanisms that lead to tryptophan starvation, chlamydial death, and eventual clearance of the bacteria (53). However, recent evidence of chlamydial reticulate bodies being able to substantially alter their gene transcription, decrease metabolism, and entering into what is known as a 'persistent' state, suggests a survival mechanism that *Chlamydia* has evolved to evade immune surveillance (54-56). Persistence in microbial infections are often implicated in the triggering of autoimmune reactions, and this was demonstrated in studies investigating the role that *Chlamydia* persistence plays in triggering self-immune reactions in infected male rodents (57).

To determine whether *Chlamydia* infection induces a cellular response that signals a state of persistence in the infected hOE cells, our multiplex analyses included several biomarkers for persistence and autoimmunity that are known to be secreted by cells in various clinical syndromes. Figures 10 and 11 show the results of the chlamydial induction of soluble CD163, chitinase-3-like 1, Lipocalin-2, osteopontin, and pentraxin-3 throughout infection in WT and TLR3 deficient hOE cells. As shown, *Chlamydia* induces the synthesis of sCD163 (a factor associated with long-term chronic inflammatory diseases such as rheumatoid arthritis) and the anti-apoptotic chitinase-3-like 1 protein in the hOE cells. However, our data show that the protein secretion levels of these biomarkers are significantly reduced in the absence of TLR3 when these cells were infected with the L2 serovar. Although secretion levels of sCD163 were much higher during infection with serovar D, there was no significant reduction during TLR3 deficiency as was observed in the L2 infection.

Figures 10 and 11 show that TLR3 deficiency leads to significantly *increased* levels of osteopontin and pentraxin-3. The role of these proteins in *Chlamydia* infection is not clear; however, osteopontin is an inflammatory mediator often associated with autoimmune disease, chronic inflammatory disorders, and progression of tumor cells (58), while pentraxin-3 is a known biomarker for pelvic inflammatory disease (PID) and is also associated with autoimmune diseases (59, 60). Collectively, our findings indicate that TLR3 may have a functional role in regulating the expression of biomarkers symbolic of long-term or persistent disease states in the *Chlamydia*-infected hOE cells, which is a precondition that often correlates with the initiation of autoimmune responses and chronic sequelae (61-64).

TLR3 deficiency altered the LPS content and size of the chlamydial inclusion.

Our previous investigations into mechanisms that impact the chlamydial-induced synthesis of IFN-β showed that disruption of IFN-β had a significant impact on the chlamydial inclusion size and chlamydial replication. In that regard, we showed that *C. muridarum* replication in murine OE cells deficient in either TLR3 or STAT-1 was more robust and that the inclusions were larger and aberrantly shaped [(15, 65); Fig S3]. To determine the physiological consequences of TLR3 deficiency on *Chlamydia* inclusion size in human oviduct epithelial tissue, we infected WT and TLR3-deficient hOE cells with *C. trachomatis*-serovar D at a MOI of 10 IFU/ cell for 36hrs. We next stained the cells for chlamydial LPS using the EVI-HI anti-*Chlamydia* LPS antibody, and examined the infected cells for chlamydial inclusion size and LPS content in fluorescent microscopy and multi-spectral flow cytometry, respectively. We first examined *C.*

526 *trachomatis*-serovar D infected hOE-WT and hOE-TLR3KO cells by immunofluorescent
527 microscopy to get a qualitative comparison of the chlamydial inclusion size in order to
528 ascertain whether TLR3 has any impact on *Chlamydia* development. As demonstrated
529 in the representative capture shown in Figure 12, we routinely saw that the chlamydial
530 inclusions in the TLR3-deficient hOE cells were much larger, amorphously shaped, and
531 were more diffusely stained with punctate patterns throughout the inclusion. In contrast,
532 the inclusions in the hOE-WT cells were generally more compact in size, more uniformly
533 stained, and had more staining intensity per pixel than the TLR3-deficient hOE cells.
534 We saw very similar trends in the *C. muridarum*-infected WT and TLR3(-) OE cells
535 derived from mice (Fig. S3).

536 We further examined *C. trachomatis*-L2 infected hOE-WT and hOE-TLR3KO
537 cells to quantitatively determine the impact of TLR3 deficiency on chlamydial inclusion
538 development and size via multi-spectral imaging flow cytometry using the Amnis Image
539 Stream X MKII. Figure 13 shows that cells deficient in TLR3 expression exhibited
540 significantly increased levels of LPS within the chlamydial inclusion, based on the
541 geometric mean fluorescence intensity differences (ΔMFI) between the two cell types.
542 The fluorescence results demonstrating increased fluorescence intensity in the hOE-
543 TLR3KO cells corroborates the IF data showing that the chlamydial inclusions were
544 larger and presumably contained more chlamydial LPS during TLR3 deficiency. Further
545 analyses of the Multi-spectral imaging flow cytometry data in IDEAS software revealed
546 that the average *Chlamydia* inclusion diameter was calculated to be 15.3μm and
547 17.2μm in the hOE-WT and hOE-TLR3KO cells, respectively. Fig. S4 shows a
548 representative image of the multi-spectral imaging flow cytometry, in which we scanned

(in triplicate) 10000 cells each of the hOE-WT and hOE-TLR3KO cells that were either mock-infected or infected with *C. trachomatis*-L2. Collectively, immunofluorescence analyses and the imaging flow cytometry results using antibody specific for chlamydial LPS indicate that TLR3 deficiency in human oviduct epithelium leads to increased chlamydial inclusion size and more LPS within the inclusion.

To examine whether *Chlamydia* replication during TLR3-deficiency correlates with the increased inclusion size and LPS content within the inclusion, we next measured chlamydial replication in wild-type and TLR3-deficient hOE cells that were infected with 5 IFU/cell *C. trachomatis*-serovar D. As shown in Figure 14, *C. trachomatis* replication was greater at all time points in the hOE-TLR3KO cells compared to the wild-type, suggesting that stimulation of TLR3 by *C. trachomatis* results in an immune response that negatively affects *Chlamydia* growth. Interestingly, our data in Figure 14 show that the chlamydial replication in hOE-WT cells peaks at around 48hr post-infection before the recovery of infectious progeny begins to drop. In contrast, the recovery of infectious EBs in the *Chlamydia*-infected hOE-TLR3KO cells continued to rise past the 48hr time point (Fig. S5). Collectively, our data indicate that TLR3 plays a role in limiting *Chlamydia* replication in the HUMAN oviduct tissue and corroborates our previous studies in mice, and thus implicate TLR3 in a protective role against genital tract *Chlamydia* infections in both species.

DISCUSSION

570 Our research focuses on the impact of TLR3 signaling on the immune response to
571 chlamydial infection in oviduct epithelium, and we were the first to demonstrate more
572 severe genital tract pathogenesis in mice deficient in TLR3 confirming our hypothesis
573 that TLR3 has a protective role in the immune responses to murine genital tract
574 infections (32). In this investigation, our goal was to ascertain whether TLR3 had a
575 similar protective role in the immune response to genital tract *Chlamydia* infection in
576 humans and to more precisely delineate those immune responses in oviduct epithelial
577 cells that contribute to the fibrosis and scarring that lead to reproductive sequelae in
578 clinical disease. The OE-E6/E7 cells used in this report were derived from human
579 Fallopian tubes and were immortalized by HPV 16 E6/E7 open reading frame (ORF) by
580 retroviral expression (26). Although these are not primary oviduct epithelial cells, the
581 cells are immortalized and offer the advantage of being able to be passaged in the
582 laboratory, and they are close enough to primary oviduct epithelial cells that they can
583 serve as an adequate representation of what we believe occurs during *in vivo*
584 *Chlamydia*-OE cell interactions during natural genital tract infection.

585 Because the OE-E6/E7 cells express a functional TLR3, we first disrupted its
586 gene expression and subsequent protein function using CRISPR to generate a TLR3-
587 deficient version of the OE-E6/E7 cells, which could then be used to help delineate
588 those immune responses to *Chlamydia* infection that are directly related to TLR3
589 function. We were able to generate several clones of the TLR3 deficient hOE cells and
590 demonstrated loss of both TLR3 protein expression and its functional response to the
591 TLR3 agonist poly (I:C). We also demonstrated a significant reduction in the chlamydial
592 induced synthesis of IFN-β in hOE cells deficient in TLR3 function; however, the

reduction was a bit more modest in the hOE-TLR3KO cells when compared to that of TLR3-deficient OE cells derived from TLR3KO mice (13). The differences that we observed in the reduction in the *Chlamydia*-induced IFN-β synthesis between the TLR3-deficient hOE and the murine OE cells are likely related to the fact that we were not able to completely disable TLR3 gene expression using CRISPR, whereas the functional TLR3 gene expression in the TLR3KO mouse is completely absent. Other possibilities to explain the more modest reduction in the *Chlamydia*-induced synthesis of IFN-β in the hOE cells could be more significant contributions of other pathways identified to enhance to the *Chlamydia*-induced type-I IFN response such as cyclic GMP–AMP (cGAMP) synthase (cGAS) and STING in the hOE cells (16, 66). The significance of the relatively higher level of IFN-β synthesis observed during *Chlamydia* infection in the TLR3-deficient hOE versus that of the TLR3-deficient murine OE cells is not yet known; however, we have shown that IFN-β can regulate the chlamydial-induced syntheses of a multitude of other inflammatory mediators (15).

As sentinels for invasion by microbial pathogens, epithelial cells lining the reproductive tract secrete cytokines and chemokines upon chlamydial infection that functions in various facets of innate immunity such as inflammation, lymphocyte recruitment, polarization, and genital tract scarring (24, 67). We have reported that TLR3 regulates the syntheses of a multitude of these factors both *in vitro* and *in vivo* in murine OE cells and mice, and concluded that TLR3 has regulatory function affecting multiple aspects of both the innate and adaptive immune response (13, 15, 32). We demonstrate in this report that TLR3 may have a similar role in human oviduct epithelial tissue and extrapolate our findings to speculate that TLR3 deficiency may have a

616 significant role in outcomes of infections in humans. As an example, we show in
617 Figures 5-7 that TLR3 deficiency in hOE cells leads to significant reductions in several
618 factors associated with the acute inflammatory response such as IL-6, IL-6Rα, sIL-6Rβ
619 (gp130) and IL-8. IL-6Rα and gp130 are the two chains that comprise the IL-6 receptor,
620 which is a type I receptor for the pleiotropic cytokine IL-6. IL-6 represents a keystone
621 cytokine in infection, cancer, and inflammation (68), and has been shown to have a
622 significant role in both inhibiting *C. muridarum* infection in mice and exacerbating its
623 pathogenicity in the mouse genital tract (69). IL-8 is a known as neutrophil chemotactic
624 factor known to be induced early during *Chlamydia* infection and was thought to be
625 associated with pre-term delivery complications in pregnant women infected with *C.*
626 *trachomatis* (70).

627 Loss of TLR3 function in the hOE cells did not result in a global down-regulation
628 in the *Chlamydia*-induced syntheses of all mediators that shape the immune response,
629 nor was its impact limited to that of the acute inflammatory response. Our data also
630 demonstrate that TLR3 deficiency leads to downregulation and *upregulation* in the
631 chlamydial-induced syntheses of several cytokines and chemokines that have an impact
632 at various phases of the adaptive immune response, which can potentially affect long-
633 term outcomes of infection in humans and impact genital tract pathology. Figures 6 and
634 7 show that the TLR3-deficient hOE cells produced significantly higher levels of the
635 leukocyte recruiting factor CCL-5 (71) and the type III interferons IL-28A and IL-29 (72)
636 when compared to WT hOE cells. The type III IFNs are hypothesized to have a role in
637 the polarization of the immune response to *Chlamydia* infection by inhibiting the
638 production of IL-13, IL-4 and IL-5, and thereby promoting the development of protective

639 Th1 immunity to infection (43). Our investigations into the role of TLR3 in the
640 pathogenesis of *C. muridarum* infection in mice show that TLR3-deficiency leads to
641 significantly altered $CD4^+/CD8^+$ T-cell ratios, and increased lymphocytic infiltration into
642 the uterine horns and oviducts by day 21 post-infection (32). The observation of
643 significantly higher levels of the type III interferons IL-28A and IL-29 in the TLR3-
644 deficient hOE cells supports a hypothesis that TLR3 may have a role in polarization of
645 the immune response in humans as well, and it would manifest itself by having an effect
646 on the recruitment of lymphocytes into the female reproductive tract in women infected
647 with *C. trachomatis*.

648 We recently reported that TLR3 deficiency resulted in an increased frequency
649 and severity in pronounced chronic sequelae (such as lymphocytic endometritis and
650 hydrosalpinx) during late stages of *C. muridarum* genital tract infections in mice (32). In
651 this report, we show that the TLR3-deficient hOE cells were dysregulated in the
652 *Chlamydia*-induced syntheses of several biomarkers associated with chronic
653 inflammation, and are suggestive that chronic clinical outcomes would occur in higher
654 frequency in humans lacking functional TLR3. Collectively, our data implicate TLR3 in
655 having some impact on regulating the incidence and severity in outcomes of chronic
656 inflammation caused during genital tract *Chlamydia* infections in humans. TNFα is
657 involved in the systemic chronic inflammation that causes many of the clinical problems
658 associated with autoimmune disorders such as rheumatoid arthritis, ankylosing
659 spondylitis, inflammatory bowel disease, psoriasis, and refractory asthma. (73-75).
660 These disorders are sometimes treated by using a TNF inhibitor, many of which that
661 either mimic the TNFα receptor (TNF-R1) to bind to and block its activity or is an actual

monoclonal antibody that binds TNFα (76). TLR3 deficiency in hOE cells showed defective syntheses of the soluble tumor necrosis factor receptor 1 (sTNF-R1) during *C. trachomatis* infection. sTNF-R1 binds to an inactivates TNFα, a major cytokine associated with scarring of oviduct tissue and severe genital tract sequelae in *C. muridarum* infected mice (44). This finding suggests that the diminished presence of sTNF-R1 in the TLR3 deficient cells would result in reduced effectiveness at inactivating *Chlamydia*-induced TNFα, and a subsequent increased incidence of TNFα-mediated scarring. In that same regard, dysregulation in the expression of matrix metalloproteinases (MMPs) is known to directly impact the severity of genital tract fibrosis and scarring in mice infected with *Chlamydia* (50-52). The *Chlamydia*-induced synthesis of MMP-1, MMP-2, MMP3, and MMP-10 was shown to be diminished in the TLR3-deficient hOE cells (Figure 9), suggesting that the normal physiological process of breaking down extracellular matrix proteins by the MMPs would be attenuated, and will likely result in increased fibrosis and scarring observed when the expression levels of certain MMPs are not sufficient (77, 78).

Our data showed that TLR3 deficiency in hOE cells significantly altered the *Chlamydia*-induced expression levels of biomarkers for chronic inflammation, persistence, and autoimmunity such as soluble CD163 (sCD163), Chitinase-3-like 1, Osteopontin (OPN), and Pentraxin-3 (58-60, 79-82). OPN was first identified in osteoclasts as an extracellular structural protein of bone and is known as an essential factor in bone remodeling (83). However, subsequent to the initial identification of OPN as a structural component of bone tissue, OPN has been shown to be expressed in a wide range of immune cells, including macrophages, neutrophils, dendritic cells, and

various lymphocyte types, and is now known to have function in several aspects of host immunity (84). The exact role that OPN plays in the immune response to *Chlamydia* infection is poorly understood; however, recent studies have linked OPN to persistent inflammation and has hypothesized a role for OPN in cell transformation during persistent *Chlamydia* infection (85, 86). Our data showing significant reductions in OPN production in the TLR3-deficient hOE cells during *C. trachomatis* infection suggest that TLR3 deficiency may lead to increased incidences of persistent infections, and proposes a role for TLR3 in the prevention of long-term chronic inflammation and possible cellular transformation. A link between sCD163, Chitinase-3-like 1, Pentraxin-3 and *Chlamydia* infection has not yet been established; however, the dysregulation of these known biomarkers for chronic inflammation, persistent infection, and autoimmunity supports a role for TLR3 in limiting the clinical symptoms of chronic inflammation during infection.

Finally, we examined the possible impact that TLR3 deficiency in hOE cells may have on chlamydial replication and inclusion structure. We previously showed that *C. muridarum* replication was more robust, the inclusions were larger and more aberrantly shaped in TLR3-deficient murine OE cells, and that TLR3-deficient mice sustained significantly higher bacterial burdens than WT mice during early and mid-infection [(15, 32); Fig. S3]. We hypothesized from those studies that the overall negative effect on *C. muridarum* biology was largely due to the host-beneficial impact of TLR3-dependent IFN-β synthesis, and we showed that chlamydial replication in TLR3-deficient OE cells pre-treated with exogenous recombinant IFN-β was significantly diminished (15). Here, we corroborate the mouse studies by showing that the inclusions were substantially

larger, and they were stained in a more punctate and diffuse pattern in TLR3-deficient hOE cells 36hrs after infection with *C. trachomatis*-serovar D. Imaging flow-cytometry revealed that TLR3-deficient hOE cells had higher levels of *Chlamydia* LPS within the chlamydial inclusion at 24hr post-infection when infected with *C. trachomatis*-L2 and are highly suggestive that the larger inclusions contain more bacterial particles. We consistently observed higher levels of *Chlamydia* replication in the TLR3-deficient hOE cells at all time-points between 24 and 72hrs post-infection (Figure 14 and Fig. S5) and that the differences were statistically significant after 48hs post-infection. Our data showing that TLR3 deficiency in hOE cells leads to the significant decreases in the chlamydial-induced synthesis of IFN-β implicates this cytokine in the control of *Chlamydia* infection in human genital tract epithelial cells as was observed in mice. However, our data in Figure 11 showed that TLR3-deficiency in hOE cells also resulted in drastic reductions in the chlamydial-induced secretion of lipocalin-2, which is an innate-immune protein that limits bacterial growth by sequestering iron-containing siderophores (87). Although it is unclear exactly which mechanism exerts the greatest impact on regulating chlamydial growth in hOE cells, our data are suggestive that there are likely redundant mechanisms that control *Chlamydia* replication that are disrupted during TLR3 deficiency.

Collectively, all of our previous investigations into the impact of TLR3 in the immune response to *Chlamydia* infection in mice have demonstrated a protective role for TLR3 in regards to genital tract pathology, and our data represents the first of such in regards to *Chlamydia* infection. Although the exact mechanism(s) that TLR3 invokes to elicit this protective immunity is unknown and needs further study, our preliminary

731 investigations implicate TLR3 function in upregulating gene expression of other TLRs
732 known to have impact on genital tract pathology (such as TLR2; (12)), through
733 pathways involving IFN-β synthesis (15). In this report, we expanded our investigations
734 into examining the impact of TLR3 in the immune response to *Chlamydia* infection in
735 human oviduct epithelial cells, and our initial results thus far show a similar role for
736 TLR3 in the protective immune response in humans. Studies are currently underway to
737 further investigate the role of this enigmatic Toll-like receptor in human genital tract
738 *Chlamydia* infection.

739

740 **ACKNOWLEDGMENTS**

741 We thank Dr. David Nelson and his lab members for providing *C. trachomatis*-L2 strain,
742 Serovar D, *Chlamydia* LPS antibody, for the use of the EVOS system, their thoughtful
743 discussion, and their support. We also thank Dr. Cheikh Seye for access to the Wes™
744 Simple Western system. We thank the Multiplex Analysis Core at Indiana University's
745 Melvin and Bren Simon Cancer Center for providing support in analyzing samples and
746 interpretation of data. This work was supported by NIH Grant AI104944 to W.A.D.

747

748 **REFERENCES**

749

750 1. **CDC** 2017, posting date. 2015 Sexually Transmitted Diseases Survey. [Online.]
751 2. **Farley TA, Cohen DA, Elkins W.** 2003. Asymptomatic sexually transmitted diseases: the case for
752 screening. Prev Med **36:**502-509.

3. **Korenromp EL, Sudaryo MK, de Vlas SJ, Gray RH, Sewankambo NK, Serwadda D, Wawer MJ, Habbema JD.** 2002. What proportion of episodes of gonorrhoea and chlamydia becomes symptomatic? Int J STD AIDS **13:**91-101.
4. **Elwell C, Mirrashidi K, Engel J.** 2016. Chlamydia cell biology and pathogenesis. Nat Rev Microbiol **14:**385-400.
5. **Nanni C, Marangoni A, Quarta C, Di Pierro D, Rizzello A, Trespidi S, D'Ambrosio D, Ambrosini V, Donati M, Aldini R, Zanotti-Fregonara P, Grassetto G, Rubello D, Fanti S, Cevenini R.** 2009. Small animal PET for the evaluation of an animal model of genital infection. Clin Physiol Funct Imaging **29:**187-192.
6. **Jerchel S, Knebel G, Konig P, Bohlmann MK, Rupp J.** 2012. A human fallopian tube model for investigation of C. trachomatis infections. J Vis Exp.
7. **Chow JM, Yonekura ML, Richwald GA, Greenland S, Sweet RL, Schachter J.** 1990. The association between Chlamydia trachomatis and ectopic pregnancy. A matched-pair, case-control study. JAMA **263:**3164-3167.
8. **Naderi T, Kazerani F, Bahraminpoor A.** 2012. Comparison of chlamydia infection prevalence between patients with and without ectopic pregnancy using the PCR method. Ginekol Pol **83:**819-821.
9. **Chen L, Lei L, Chang X, Li Z, Lu C, Zhang X, Wu Y, Yeh IT, Zhong G.** 2010. Mice deficient in MyD88 Develop a Th2-dominant response and severe pathology in the upper genital tract following Chlamydia muridarum infection. J Immunol **184:**2602-2610.
10. **Stephens RS.** 2003. The cellular paradigm of chlamydial pathogenesis. Trends Microbiol **11:**44-51.
11. **Bakken TE, Roddey JC, Djurovic S, Akshoomoff N, et, al.,.** 2012. Association of common genetic variants in GPCPD1 with scaling of visual cortical surface area in humans. Proceedings of the National Academy of Sciences of the United States of America **109:**3985-3990.
12. **Darville T, O'Neill JM, Andrews CW, Jr., Nagarajan UM, Stahl L, Ojcius DM.** 2003. Toll-like receptor-2, but not Toll-like receptor-4, is essential for development of oviduct pathology in chlamydial genital tract infection. J Immunol **171:**6187-6197.
13. **Derbigny WA, Johnson RM, Toomey KS, Ofner S, Jayarapu K.** 2010. The Chlamydia muridarum-induced IFN-beta response is TLR3-dependent in murine oviduct epithelial cells. J Immunol **185:**6689-6697.
14. **Derbigny WA, Kerr MS, Johnson RM.** 2005. Pattern recognition molecules activated by Chlamydia muridarum infection of cloned murine oviduct epithelial cell lines. J Immunol **175:**6065-6075.
15. **Derbigny WA, Shobe LR, Kamran JC, Toomey KS, Ofner S.** 2012. Identifying a role for Toll-like receptor 3 in the innate immune response to Chlamydia muridarum infection in murine oviduct epithelial cells. Infection and immunity **80:**254-265.
16. **Prantner D, Darville T, Nagarajan UM.** 2010. Stimulator of IFN gene is critical for induction of IFN-beta during Chlamydia muridarum infection. J Immunol **184:**2551-2560.
17. **Rank RG, Lacy HM, Goodwin A, Sikes J, Whittimore J, Wyrick PB, Nagarajan UM.** 2010. Host chemokine and cytokine response in the endocervix within the first developmental cycle of Chlamydia muridarum. Infection and immunity **78:**536-544.
18. **Welter-Stahl L, Ojcius DM, Viala J, Girardin S, Liu W, Delarbre C, Philpott D, Kelly KA, Darville T.** 2006. Stimulation of the cytosolic receptor for peptidoglycan, Nod1, by infection with Chlamydia trachomatis or Chlamydia muridarum. Cell Microbiol **8:**1047-1057.
19. **Da Costa CU, Wantia N, Kirschning CJ, Busch DH, Rodriguez N, Wagner H, Miethke T.** 2004. Heat shock protein 60 from Chlamydia pneumoniae elicits an unusual set of inflammatory responses via Toll-like receptor 2 and 4 in vivo. European journal of immunology **34:**2874-2884.

20. **Erridge C, Pridmore A, Eley A, Stewart J, Poxton IR.** 2004. Lipopolysaccharides of Bacteroides fragilis, Chlamydia trachomatis and Pseudomonas aeruginosa signal via toll-like receptor 2. J Med Microbiol **53:**735-740.
21. **Netea MG, Kullberg BJ, Galama JM, Stalenhoef AF, Dinarello CA, Van der Meer JW.** 2002. Non-LPS components of Chlamydia pneumoniae stimulate cytokine production through Toll-like receptor 2-dependent pathways. European journal of immunology **32:**1188-1195.
22. **Prebeck S, Kirschning C, Durr S, da Costa C, Donath B, Brand K, Redecke V, Wagner H, Miethke T.** 2001. Predominant role of toll-like receptor 2 versus 4 in Chlamydia pneumoniae-induced activation of dendritic cells. J Immunol **167:**3316-3323.
23. **Aziz A.** 2006. A study on immunopathogenetic mechanisms of atherosclerotic process caused by chronic infection of Chlamydia pneumoniae in rats (Ratus novergicus). Acta Med Indones **38:**206-212.
24. **Johnson RM.** 2004. Murine oviduct epithelial cell cytokine responses to Chlamydia muridarum infection include interleukin-12-p70 secretion. Infection and immunity **72:**3951-3960.
25. **Li HW, Liao SB, Chiu PC, Tam WW, Ho JC, Ng EH, Ho PC, Yeung WS, Tang F, O WS.** 2010. Expression of adrenomedullin in human oviduct, its regulation by the hormonal cycle and contact with spermatozoa, and its effect on ciliary beat frequency of the oviductal epithelium. J Clin Endocrinol Metab **95:**E18-25.
26. **Lee YL, Lee KF, Xu JS, Wang YL, Tsao SW, Yeung WS.** 2001. Establishment and characterization of an immortalized human oviductal cell line. Molecular reproduction and development **59:**400-409.
27. **Zandieh Z, Ashrafi M, Jameie B, Amanpour S, Mosaffa N, Salman Yazdi R, Pacey A, Aflatoonian R.** 2015. Evaluation of immunological interaction between spermatozoa and fallopian tube epithelial cells. Andrologia **47:**1120-1130.
28. **Shaw JL, Wills GS, Lee KF, Horner PJ, McClure MO, Abrahams VM, Wheelhouse N, Jabbour HN, Critchley HO, Entrican G, Horne AW.** 2011. Chlamydia trachomatis infection increases fallopian tube PROKR2 via TLR2 and NFkappaB activation resulting in a microenvironment predisposed to ectopic pregnancy. Am J Pathol **178:**253-260.
29. **Nagarajan UM, Ojcius DM, Stahl L, Rank RG, Darville T.** 2005. Chlamydia trachomatis induces expression of IFN-gamma-inducible protein 10 and IFN-beta independent of TLR2 and TLR4, but largely dependent on MyD88. J Immunol **175:**450-460.
30. **O'Connell CM, Ionova IA, Quayle AJ, Visintin A, Ingalls RR.** 2006. Localization of TLR2 and MyD88 to Chlamydia trachomatis inclusions. Evidence for signaling by intracellular TLR2 during infection with an obligate intracellular pathogen. The Journal of biological chemistry **281:**1652-1659.
31. **Yang X, Coriolan D, Schultz K, Golenbock DT, Beasley D.** 2005. Toll-like receptor 2 mediates persistent chemokine release by Chlamydia pneumoniae-infected vascular smooth muscle cells. Arteriosclerosis, thrombosis, and vascular biology **25:**2308-2314.
32. **Carrasco SE, Hu S, Imai DM, Kumar R, Sandusky GE, Yang XF, Derbigny WA.** 2018. Toll-like receptor 3 (TLR3) promotes the resolution of Chlamydia muridarum genital tract infection in congenic C57BL/6N mice. PLoS One **13:**e0195165.
33. **Brothwell JA, Muramatsu MK, Toh E, Rockey DD, Putman TE, Barta ML, Hefty PS, Suchland RJ, Nelson DE.** 2016. Interrogating Genes That Mediate Chlamydia trachomatis Survival in Cell Culture Using Conditional Mutants and Recombination. Journal of bacteriology **198:**2131-2139.
34. **Skovdahl HK, Granlund AvB, Østvik AE, Bruland T, Bakke I, Torp SH, Damås JK, Sandvik AK.** 2015. Expression of CCL20 and Its Corresponding Receptor CCR6 Is Enhanced in Active Inflammatory Bowel Disease, and TLR3 Mediates CCL20 Expression in Colonic Epithelial Cells. PloS one **10:**e0141710-e0141710.

35. **Matsumoto M, Funami K, Tanabe M, Oshiumi H, Shingai M, Seto Y, Yamamoto A, Seya T.** 2003. Subcellular localization of Toll-like receptor 3 in human dendritic cells. J Immunol **171:**3154-3162.
36. **Matsumoto M, Kikkawa S, Kohase M, Miyake K, Seya T.** 2002. Establishment of a monoclonal antibody against human Toll-like receptor 3 that blocks double-stranded RNA-mediated signaling. Biochemical and biophysical research communications **293:**1364-1369.
37. **Carpenter S, O'Neill LA.** 2009. Recent insights into the structure of Toll-like receptors and post-translational modifications of their associated signalling proteins. Biochem J **422:**1-10.
38. **Derbigny WA, Hong SC, Kerr MS, Temkit M, Johnson RM.** 2007. Chlamydia muridarum infection elicits a beta interferon response in murine oviduct epithelial cells dependent on interferon regulatory factor 3 and TRIF. Infection and immunity **75:**1280-1290.
39. **Cheng W, Shivshankar P, Li Z, Chen L, Yeh IT, Zhong G.** 2008. Caspase-1 contributes to Chlamydia trachomatis-induced upper urogenital tract inflammatory pathologies without affecting the course of infection. Infection and immunity **76:**515-522.
40. **Darville T, Andrews CW, Jr., Sikes JD, Fraley PL, Rank RG.** 2001. Early local cytokine profiles in strains of mice with different outcomes from chlamydial genital tract infection. Infection and immunity **69:**3556-3561.
41. **Maxion HK, Kelly KA.** 2002. Chemokine expression patterns differ within anatomically distinct regions of the genital tract during Chlamydia trachomatis infection. Infection and immunity **70:**1538-1546.
42. **Tseng CT, Rank RG.** 1998. Role of NK cells in early host response to chlamydial genital infection. Infection and immunity **66:**5867-5875.
43. **Wan C, Latter JL, Amirshahi A, Symonds I, Finnie J, Bowden N, Scott RJ, Cunningham KA, Timms P, Beagley KW.** 2014. Progesterone activates multiple innate immune pathways in Chlamydia trachomatis-infected endocervical cells. Am J Reprod Immunol **71:**165-177.
44. **Murthy AK, Li W, Chaganty BK, Kamalakaran S, Guentzel MN, Seshu J, Forsthuber TG, Zhong G, Arulanandam BP.** 2011. Tumor necrosis factor alpha production from CD8+ T cells mediates oviduct pathological sequelae following primary genital Chlamydia muridarum infection. Infection and immunity **79:**2928-2935.
45. **Schneider P, MacKay F, Steiner V, Hofmann K, Bodmer JL, Holler N, Ambrose C, Lawton P, Bixler S, Acha-Orbea H, Valmori D, Romero P, Werner-Favre C, Zubler RH, Browning JL, Tschopp J.** 1999. BAFF, a novel ligand of the tumor necrosis factor family, stimulates B cell growth. J Exp Med **189:**1747-1756.
46. **Igietseme JU, Omosun Y, Nagy T, Stuchlik O, Reed MS, He Q, Partin J, Joseph K, Ellerson D, George Z, Goldstein J, Eko FO, Bandea C, Pohl J, Black CM.** 2018. Molecular Pathogenesis of Chlamydia Disease Complications: Epithelial-Mesenchymal Transition and Fibrosis. Infection and immunity **86**.
47. **Nagase H, Woessner JF, Jr.** 1999. Matrix metalloproteinases. The Journal of biological chemistry **274:**21491-21494.
48. **Ault KA, Kelly KA, Ruther PE, Izzo AA, Izzo LS, Sigar IM, Ramsey KH.** 2002. Chlamydia trachomatis enhances the expression of matrix metalloproteinases in an in vitro model of the human fallopian tube infection. American journal of obstetrics and gynecology **187:**1377-1383.
49. **El-Asrar AM, Geboes K, Al-Kharashi SA, Al-Mosallam AA, Missotten L, Paemen L, Opdenakker G.** 2000. Expression of gelatinase B in trachomatous conjunctivitis. Br J Ophthalmol **84:**85-91.
50. **Imtiaz MT, Distelhorst JT, Schripsema JH, Sigar IM, Kasimos JN, Lacy SR, Ramsey KH.** 2007. A role for matrix metalloproteinase-9 in pathogenesis of urogenital Chlamydia muridarum infection in mice. Microbes Infect **9:**1561-1566.

51. **Imtiaz MT, Schripsema JH, Sigar IM, Kasimos JN, Ramsey KH.** 2006. Inhibition of matrix metalloproteinases protects mice from ascending infection and chronic disease manifestations resulting from urogenital Chlamydia muridarum infection. Infection and immunity **74:**5513-5521.
52. **Pal S, Schmidt AP, Peterson EM, Wilson CL, de la Maza LM.** 2006. Role of matrix metalloproteinase-7 in the modulation of a Chlamydia trachomatis infection. Immunology **117:**213-219.
53. **Brunham RC, Rey-Ladino J.** 2005. Immunology of Chlamydia infection: implications for a Chlamydia trachomatis vaccine. Nature reviews. Immunology **5:**149-161.
54. **Witkin SS, Minis E, Athanasiou A, Leizer J, Linhares IM.** 2017. Chlamydia trachomatis: the Persistent Pathogen. Clin Vaccine Immunol **24**.
55. **Beatty WL, Belanger TA, Desai AA, Morrison RP, Byrne GI.** 1994. Tryptophan depletion as a mechanism of gamma interferon-mediated chlamydial persistence. Infection and immunity **62:**3705-3711.
56. **Beatty WL, Byrne GI, Morrison RP.** 1993. Morphologic and antigenic characterization of interferon gamma-mediated persistent Chlamydia trachomatis infection in vitro. Proceedings of the National Academy of Sciences of the United States of America **90:**3998-4002.
57. **Mackern-Oberti JP, Motrich RD, Breser ML, Cejas H, Cuffini C, Maccioni M, Rivero VE.** 2011. Male rodent genital tract infection with Chlamydia muridarum: persistence in the prostate gland that triggers self-immune reactions in genetically susceptible hosts. J Urol **186:**1100-1106.
58. **Rittling SR, Singh R.** 2015. Osteopontin in Immune-mediated Diseases. J Dent Res **94:**1638-1645.
59. **Huang XL, Zhang L, Duan Y, Wang YJ, Wang J.** 2016. Association of Pentraxin 3 with Autoimmune Diseases: A Systematic Review and Meta-Analysis. Arch Med Res **47:**223-231.
60. **Yang SF, Wu TF, Tsai HT, Lin LY, Wang PH.** 2014. New markers in pelvic inflammatory disease. Clin Chim Acta **431:**118-124.
61. **Baio P, Brucato A, Buskila D, Gershwin ME, Giacomazzi D, Lopez LR, Luzzati R, Matsuura E, Selmi C, Sarzi-Puttini P, Atzeni F, Kessel A, Toubi E.** 2008. Autoimmune diseases and infections: controversial issues Chronic HCV-related autoimmunity: a consequence of viral persistence and lymphotropism. Clin Exp Rheumatol **26:**S74-80.
62. **Teixeira AR, Hecht MM, Guimaro MC, Sousa AO, Nitz N.** 2011. Pathogenesis of chagas' disease: parasite persistence and autoimmunity. Clin Microbiol Rev **24:**592-630.
63. **Dolcino M, Puccetti A, Barbieri A, Bason C, Tinazzi E, Ottria A, Patuzzo G, Martinelli N, Lunardi C, Kung TN, Bykerk VP, Teixeira AR, Hecht MM, Guimaro MC, Sousa AO, Nitz N.** 2015. Infections and autoimmunity: role of human cytomegalovirus in autoimmune endothelial cell damage Detecting the earliest signs of rheumatoid arthritis: symptoms and examination Pathogenesis of chagas' disease: parasite persistence and autoimmunity. Lupus **24:**419-432.
64. **Sebastiani GD, Galeazzi M, Baio P, Brucato A, Buskila D, Gershwin ME, Giacomazzi D, Lopez LR, Luzzati R, Matsuura E, Selmi C, Sarzi-Puttini P, Atzeni F, Kessel A, Toubi E.** 2009. Infection--genetics relationship in systemic lupus erythematosusAutoimmune diseases and infections: controversial issues Chronic HCV-related autoimmunity: a consequence of viral persistence and lymphotropism. Lupus **18:**1169-1175.
65. **Hosey KL, Hu S, Derbigny WA.** 2015. Role of STAT1 in Chlamydia-Induced Type-1 Interferon Production in Oviduct Epithelial Cells. J Interferon Cytokine Res **35:**901-916.
66. **Zhang Y, Yeruva L, Marinov A, Prantner D, Wyrick PB, Lupashin V, Nagarajan UM.** 2014. The DNA sensor, cyclic GMP-AMP synthase, is essential for induction of IFN-beta during Chlamydia trachomatis infection. J Immunol **193:**2394-2404.

67. **Kagnoff MF, Eckmann L.** 1997. Epithelial cells as sensors for microbial infection. The Journal of clinical investigation **100:**6-10.
68. **Hunter CA, Jones SA.** 2015. IL-6 as a keystone cytokine in health and disease. Nat Immunol **16:**448-457.
69. **Sun X, Tian Q, Wang L, Xue M, Zhong G.** 2017. IL-6-mediated signaling pathways limit Chlamydia muridarum infection and exacerbate its pathogenicity in the mouse genital tract. Microbes Infect **19:**536-545.
70. **Vogel I, Thorsen P, Curry A, Sandager P, Uldbjerg N.** 2005. Biomarkers for the prediction of preterm delivery. Acta Obstet Gynecol Scand **84:**516-525.
71. **Maghazachi AA, Al-Aoukaty A, Schall TJ.** 1996. CC chemokines induce the generation of killer cells from CD56+ cells. European journal of immunology **26:**315-319.
72. **Li M, Liu X, Zhou Y, Su SB.** 2009. Interferon-lambdas: the modulators of antivirus, antitumor, and immune responses. J Leukoc Biol **86:**23-32.
73. **Billmeier U, Dieterich W, Neurath MF, Atreya R.** 2016. Molecular mechanism of action of anti-tumor necrosis factor antibodies in inflammatory bowel diseases. World J Gastroenterol **22:**9300-9313.
74. **Deodhar A, Yu D, Mantravadi S, Ogdie A, Kraft WK.** 2017. Switching tumor necrosis factor inhibitors in the treatment of axial spondyloarthritis

Tumor necrosis factor inhibitors in psoriatic arthritis. Semin Arthritis Rheum **47:**343-350.

75. **Kalden JR, Schulze-Koops H, Prado MS, Bendtzen K, Andrade LEC, Cohen BL, Sachar DB, Chang R, Yee KL, Sumbria RK.** 2017. Immunogenicity and loss of response to TNF inhibitors: implications for rheumatoid arthritis treatment Biological anti-TNF drugs: immunogenicity underlying treatment failure and adverse eventsUpdate on anti-tumor necrosis factor agents and other new drugs for inflammatory bowel disease

Tumor necrosis factor alpha Inhibition for Alzheimer's Disease. Nat Rev Rheumatol **13:**707-718.

76. **Haraoui B, Bykerk V.** 2007. Etanercept in the treatment of rheumatoid arthritis. Ther Clin Risk Manag **3:**99-105.
77. **Lee DE, Trowbridge RM, Ayoub NT, Agrawal DK.** 2015. High-mobility Group Box Protein-1, Matrix Metalloproteinases, and Vitamin D in Keloids and Hypertrophic Scars. Plast Reconstr Surg Glob Open **3:**e425.
78. **Rohani MG, Parks WC, Lee DE, Trowbridge RM, Ayoub NT, Agrawal DK.** 2015. Matrix remodeling by MMPs during wound repair High-mobility Group Box Protein-1, Matrix Metalloproteinases, and Vitamin D in Keloids and Hypertrophic Scars. Matrix Biol **44-46:**113-121.
79. **Kirkegaard-Klitbo DM, Mejer N, Knudsen TB, Moller HJ, Moestrup SK, Poulsen SD, Kronborg G, Benfield T.** 2017. Soluble CD163 predicts incident chronic lung, kidney and liver disease in HIV infection. AIDS **31:**981-988.
80. **Zhi Y, Gao P, Xin X, Li W, Ji L, Zhang L, Zhang X, Zhang J.** 2017. Clinical significance of sCD163 and its possible role in asthma (Review). Mol Med Rep **15:**2931-2939.
81. **Di Rosa M, Distefano G, Zorena K, Malaguarnera L.** 2016. Chitinases and immunity: Ancestral molecules with new functions. Immunobiology **221:**399-411.
82. **Nathan N, Corvol H, Amselem S, Clement A, Di Rosa M, Malaguarnera L, Di Rosa M, Distefano G, Zorena K, Malaguarnera L.** 2015. Biomarkers in Interstitial lung diseases Chitinase 3 Like-1: An Emerging Molecule Involved in Diabetes and Diabetic Complications Chitinases and immunity: Ancestral molecules with new functions. Paediatr Respir Rev **16:**219-224.

83. **Choi ST, Kim JH, Kang EJ, Lee SW, Park MC, Park YB, Lee SK.** 2008. Osteopontin might be involved in bone remodelling rather than in inflammation in ankylosing spondylitis. Rheumatology (Oxford) **47:**1775-1779.

84. **Wang KX, Denhardt DT.** 2008. Osteopontin: role in immune regulation and stress responses. Cytokine Growth Factor Rev **19:**333-345.

85. **De Filippis A, Buommino E, Domenico MD, Feola A, Brunetti-Pierri R, Rizzo A, Rizzo A, Carratelli CR, De Filippis A, Bevilacqua N, Tufano MA, Buommino E.** 2017. Chlamydia trachomatis induces an upregulation of molecular biomarkers podoplanin, Wilms' tumour gene 1, osteopontin and inflammatory cytokines in human mesothelial cells Transforming activities of Chlamydia pneumoniae in human mesothelial cells. Microbiology **163:**654-663.

86. **Rizzo A, Carratelli CR, De Filippis A, Bevilacqua N, Tufano MA, Buommino E.** 2014. Transforming activities of Chlamydia pneumoniae in human mesothelial cells. Int Microbiol **17:**185-193.

87. **Flo TH, Smith KD, Sato S, Rodriguez DJ, Holmes MA, Strong RK, Akira S, Aderem A.** 2004. Lipocalin 2 mediates an innate immune response to bacterial infection by sequestrating iron. Nature **432:**917-921.

Figure Legends

FIGURE 1. TLR3 is present and functional in human OE-E6/7 cells. Human OE-E6/7 cells were seeded in 12 well plates and cultured in DMEM only, or DMEM supplemented with either poly (I:C) for 24hrs or infected with 10 IFU/ cell *C. trachomatis*-L2 for 36hrs. (A) Poly (I:C) induced the expression of IFN-β mRNA in a dose-dependent manner. Relative expression of (B) IFN-β mRNA and (C) TLR3 mRNA in response to *C. trachomatis*-L2 infection at the time-point indicated. Data are representative of at least three independent experiments.

FIGURE 2. Disruption of TLR3 protein expression in human oviduct and cervical cells. Wes™ simple western system was used to confirm the disruption of TLR3 protein expression: (A) Human OE-E6/7 cells. Lane 1, Ladder; lane 2, 400ng WT human OE-E6/7 cell protein; lane 3, 400ng hOE-TLR3KO cell protein. (B) Hela cells. Lane 1, Ladder; lane 2, 400ng WT Hela cell protein; lane 3, 400ng Hela-TLR3KO cell protein. Data presented are representative data of selected TLR3-deficient clones from both cell types.

FIGURE 3. Disruption of TLR3 function by CRISPR dramatically decreases IFN-β mRNA expression in response to poly (I:C) stimulation. Selected clones representing TLR3-deficient: (A) Oviduct [hOE] and (B) Cervical [Hela] cells were treated with 0, 25, 50, 100 µg/mL poly (I:C) for 24hrs. The cells were harvested for total

cell RNA isolation. The response to poly (I:C) was determined by measuring the induction of IFN-β mRNA synthesis via qPCR. The relative gene expression levels of each clone compared to their respective non-target CRISPR controls are shown. Data are representative of at least three independent experiments.

FIGURE 4. TLR3 deficiency results in the decreased synthesis of IFN-β during *C. trachomatis* infection of oviduct epithelium. (A) WT and TLR3-deficient hOE cells were either mock infected or infected with *C. trachomatis*-L2 at a MOI 10 IFU/ cell for up to 36hrs. Supernatants were collected from cells representing mock, 18h, and 36h post-infection before measuring the chlamydial induced synthesis of IFN-β by standard ELISA. (B) WT hOE cells were infected with 10 IFU/cell *C. trachomatis*-L2 24hrs after treatment with 2.5 µg/ml of either si-SCR or TLR3-specific siRNA (si-TLR3). Supernatants were harvested at 24hrs post-infection to measure the chlamydial induced synthesis of IFN-β by standard ELISA. (C) CLUSTAL-O multiple sequence alignment of a sequenced PCR product containing exon #2 of human TLR3 reveal early stop codon (TGA) at position 141. The TGA stop codon is inside the red box, and gRNA sequences are highlighted with a green line. Data are representative of at least 3 independent experiments. Statistically significant differences are shown by asterisks (***, $p<0.005$).

FIGURE 5. TLR3 deficiency results in the attenuation of many of the acute-phase inflammatory mediators. WT and TLR3-deficient hOE cells were infected with *C. trachomatis*-L2 at a MOI 10 IFU/ cell for up to 30hrs. Supernatants were collected from individual wells every 6 hours for multiplex ELISA analyses to measure the expression of: (A) IL-6Ra; (B) sIL-6Rβ (gp130), (C) IL-8, (D) IL-20, (E) IL-26, and (F) IL-34. Statistically significant differences are shown by asterisks (**, p<0.01; ***, p<0.001). Data are representative of three independent experiments.

FIGURE 6. TLR3 deficiency alters the acute-phase inflammatory mediator synthesis during infection with *C. trachomatis*-serovar D**.** WT and TLR3-deficient hOE cells were infected with *C. trachomatis*-serovar D at a MOI 10 IFU/ cell for up to 72hrs. Supernatants were collected from individual wells at the time listed for multiplex ELISA analyses to measure the expression of: (A) IL-6, (B) IL-6Rα, (C) sIL-6Rβ (gp130), (D) IL-8, and (E) CCL5. Statistically significant differences are shown by asterisks (*, p<0.05; **, p<0.01; ***, p<0.005). Data are representative of three independent experiments.

FIGURE 7. TLR3 deficiency causes the increased expression of type-III IFNs. WT and TLR3-deficient hOE cells were infected with *C. trachomatis*-L2 at a MOI 10 IFU/ cell for up to 30hrs. Supernatants were collected from individual wells every 6 hours for multiplex ELISA analyses to measure the expression of: (A) IL-29 and (B) IL-28A.

Statistically significant differences are shown by asterisks (**, p<0.01; ***, p<0.001). Data are representative of three independent experiments.

FIGURE 8. TLR3 deficiency alters the synthesis of cytokines associated with cellular adhesion and tissue integrity during genital tract infection with *C. trachomatis*. WT and TLR3-deficient hOE cells were infected with either *C. trachomatis*-L2 (**A-B**) or *C. trachomatis*-serovar D (**C-E**) at a MOI 10 IFU/ cell for up to 72hrs. Supernatants were collected from individual wells at the time listed for multiplex ELISA analyses to measure the expression of: (**A, D**) sTNF-R1, (**B**) (TNFSF13B), (**C**) TGF-β1, and (**E**) ICAM-1. Statistically significant differences are shown by asterisks (*, p<0.05; **, p<0.01; ***, p<0.005). Data are representative of three independent experiments.

FIGURE 9. TLR3 regulates the *Chlamydia*-induced expression of matrix metalloproteinases during genital tract infections with *C. trachomatis*. WT and TLR3-deficient hOE cells were infected with 10 IFU/ cell with either *C. trachomatis*-L2 (**A-C**) or *C. trachomatis*-serovar D (**D-F**) for up to 72hrs. Supernatants were collected from individual wells at the time listed for multiplex ELISA analyses to measure the expression of: (**A, D**) MMP-1, (**B**) MMP-2 (**C, E**) MMP-3, and (**F**) MMP-10. Statistically significant differences are shown by asterisks (*, p<0.05; **, p<0.01; ***, p<0.005). Data are representative of three independent experiments.

FIGURE 10. TLR3 plays a role in regulating the *Chlamydia*-induced syntheses of biomarkers associated with persistence and autoimmunity. Secreted protein levels of (A) sCD163, (B) Chitinase-3-like 1, (C) Osteopontin, and (D) Pentraxin-3 were measured in the supernatants of WT and TLR3-deficient hOE cells that were infected with *C. trachomatis*-L2 at a MOI 10 IFU/ cell for up to 30hrs. The supernatants were collected from individual wells for multiplex ELISA analyses at the listed time point post-infection. Statistically significant differences are denoted by asterisks (***, $p<0.001$). Data are representative of three independent experiments.

FIGURE 11. TLR3 plays a role in regulating the *Chlamydia*-induced syntheses of biomarkers associated with iron sequestration, persistence, and autoimmunity during infection with *C. trachomatis*-serovar D**.** WT and TLR3-deficient hOE cells were infected with *C. trachomatis*-serovar D at a MOI 10 IFU/ cell for up to 72hrs. Supernatants were collected from individual wells at the time listed for multiplex ELISA analyses to measure the expression of: (A) sCD163, (B) Lipocalin-2, (C) Osteopontin, and (D) Pentraxin-3. Statistically significant differences are shown by asterisks (*, $p<0.05$; ***, $p<0.005$; ****, $p<0.001$). Data are representative of three independent experiments.

Figure 12. TLR3 deficiency in murine OE cells leads to larger and aberrantly shaped chlamydial inclusions. hOE-WT cells (A and B) and hOE-TLR3KO cells (C and D) were either mock treated or infected with *C. trachomatis*-serovar D at a MOI of

10 IFU/ cell for 36hrs. The chlamydial inclusion was stained using anti-chlamydial LPS monoclonal antibody and detected via Alexa-fluor 488 conjugated secondary antibody. Nuclei were visualized via DAPI staining (panels B and D). *Data shown are representative. Arrows show smaller vs. larger inclusion; magnification 60x.*

FIGURE 13. LPS levels within the chlamydial inclusions of infected WT and TLR3-deficient hOE cells. hOE-WT and hOE-TLR3KO cells were either mock treated or infected with *C. trachomatis*-L2 (in triplicate) at MOI of 5 IFU/ cell for 72hrs. *Chlamydia* LPS levels were determined in multispectral flow cytometric analyses of hOE cells stained using anti-*Chlamydia* LPS monoclonal antibody and allophycocyanin (APC) conjugated secondary antibody. APC-conjugated anti-IgG served as an isotype staining control. 10000 cells/events were processed in flow cytometry analysis. ΔMFI, Δ Geometric Mean Fluorescent Intensity. Data shown are representative of three independent experiments. Statistically significant differences are shown by asterisks (**, $p<0.01$).

FIGURE 14. Measuring chlamydial replication in infected WT and TLR3-deficient hOE cells. hOE-WT and hOE-TLR3KO cells were either mock treated or infected with *C. trachomatis*-serovar D (in triplicate) at MOI of 5 IFU/ cell for 72hrs. The cells were disrupted in SPG buffer at the indicated time points as described in Materials and Methods and lysates were collected, sonicated, and titered on fresh Hela cell monolayers. The data presented are representative of three different experiments.

Statistically significant differences are shown by asterisks (***, $p<0.005$; ****, $p<0.001$). IFU, inclusion forming units.

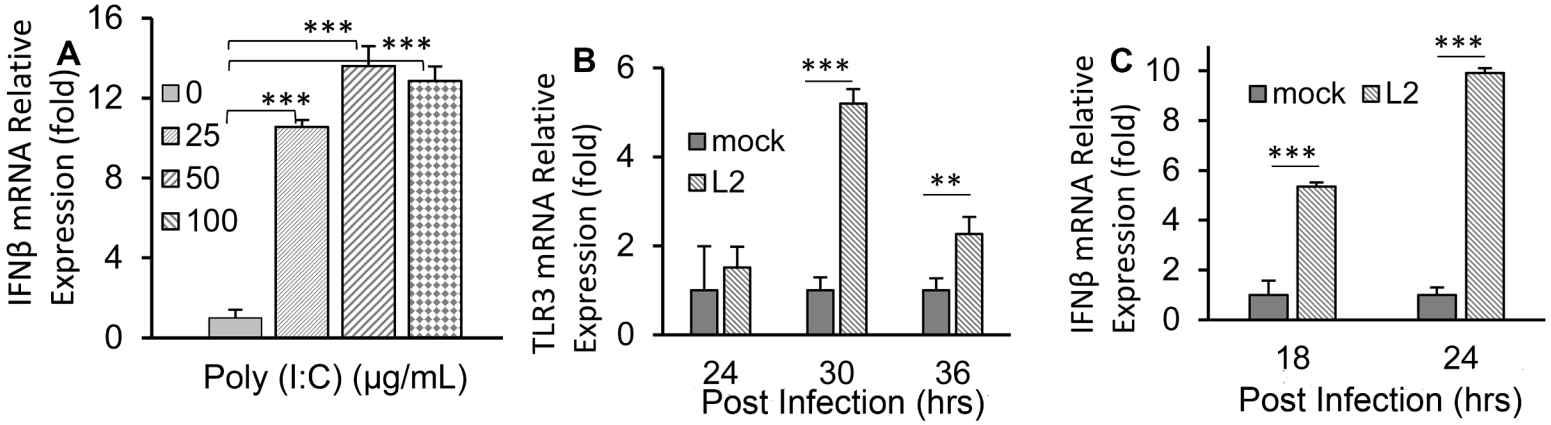

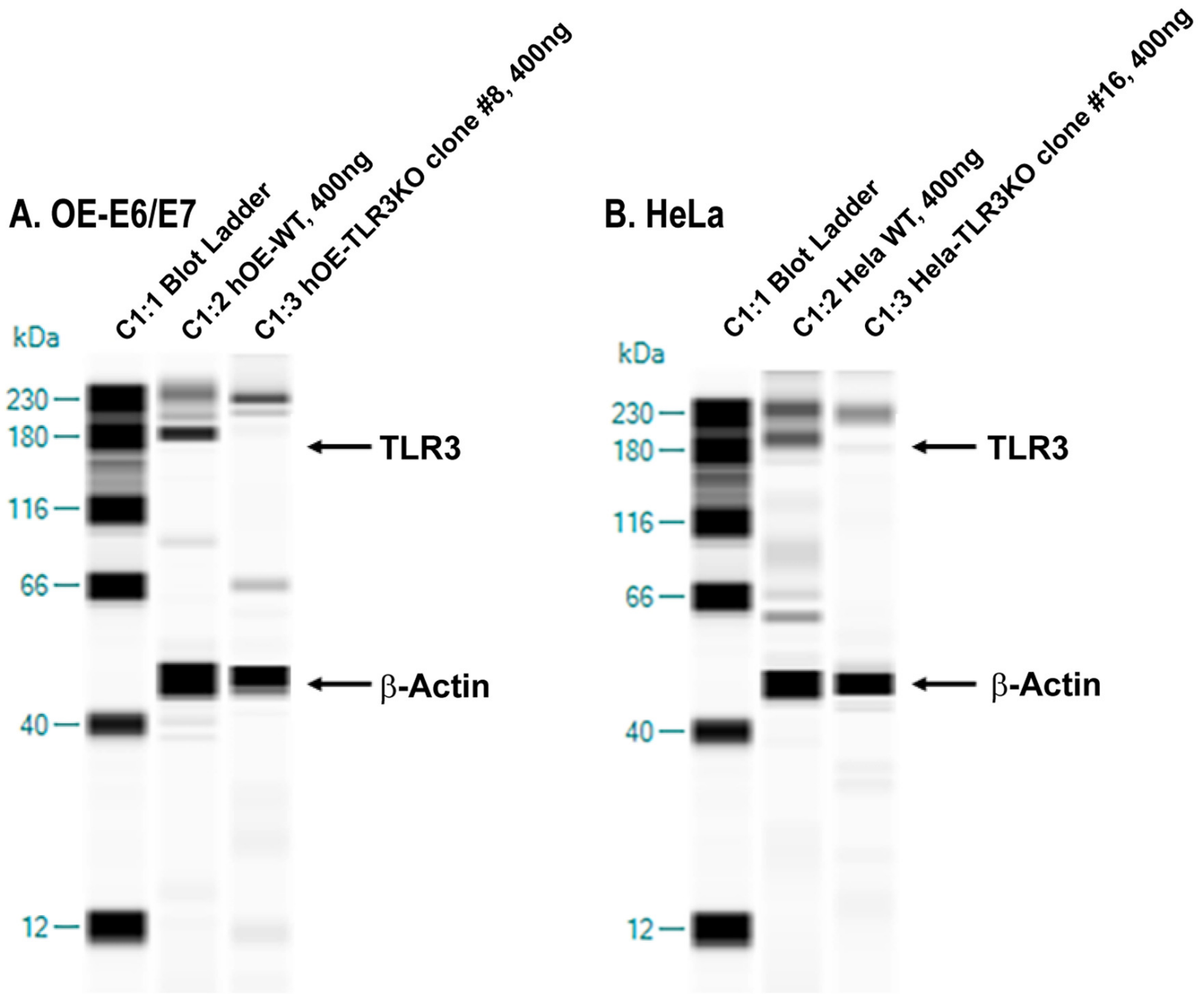

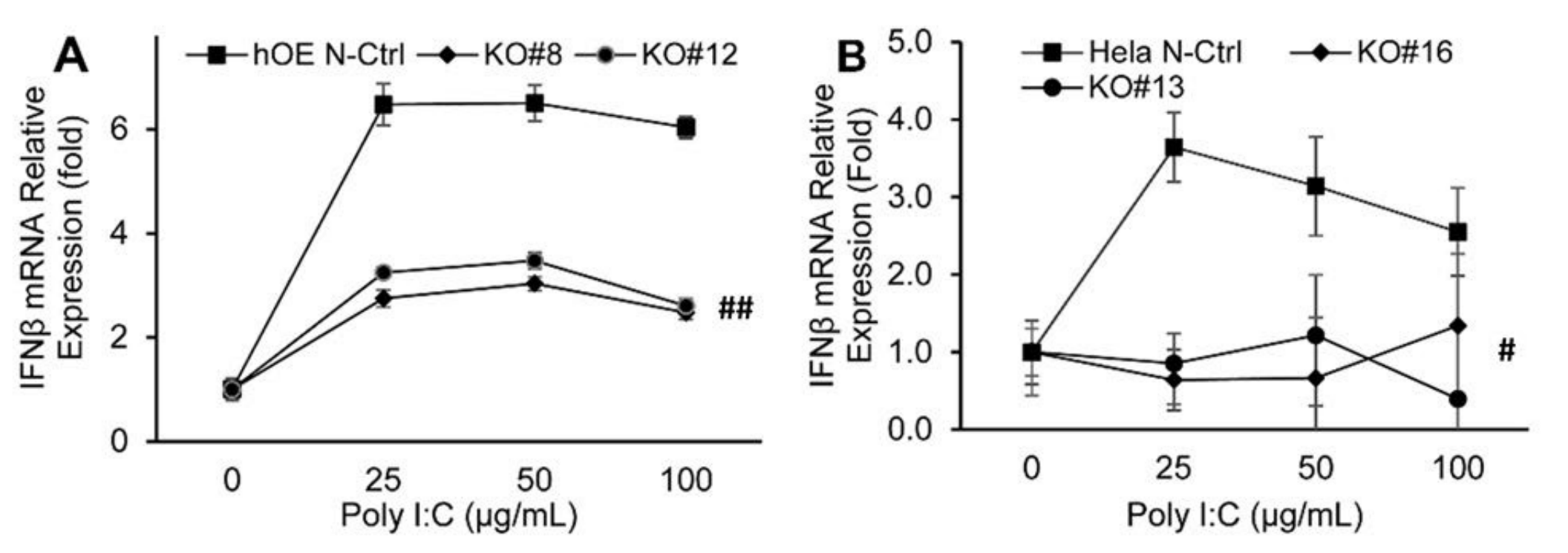
A
hOE N-Ctrl
KO#8
KO#12
IFNβ mRNA Relative Expression (fold)
0
2
4
6
0
25
50
100
Poly I:C (μg/mL)
##
B
Hela N-Ctrl
KO#16
KO#13
IFNβ mRNA Relative Expression (Fold)
0.0
1.0
2.0
3.0
4.0
5.0
0
25
50
100
Poly I:C (μg/mL)
#

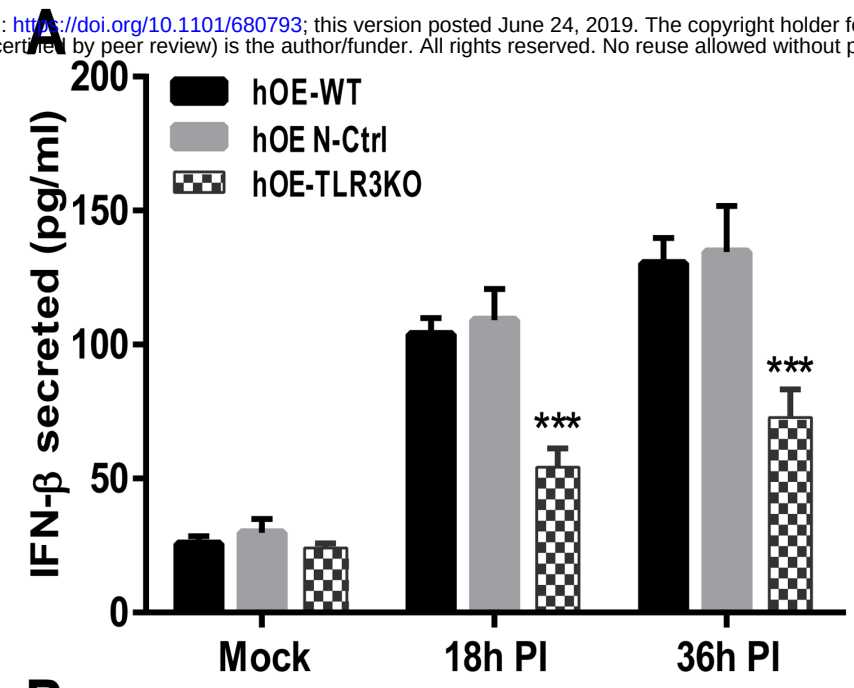

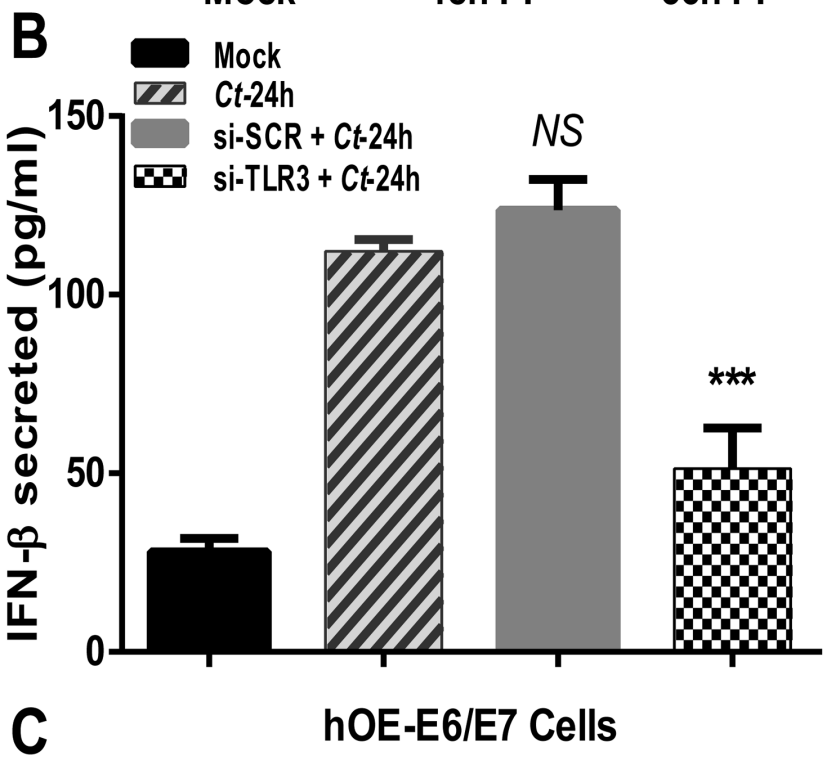

C

CLUSTAL O(1.2.4) multiple sequence alignment

```
HOE-E6/E7-WT-Exon2          ATGAGACAGACTTTGCCTTGTATCTACTTTTGGGGGGGCCTTTTGCCCTTTGGGATGCTG      60
HOE-E6/E7-shTLR3-Exon2      ATGAGACAGACTTTGCCTTGTATCTACTTTTGGGGGGGCCTTTTGCCCTTTGGGATGCTG      60
                            ************************************************************

HOE-E6/E7-WT-Exon2          TGTGCATCCTCCACCACCAAGTGCACTGTTAGCCATGAAGTTGCTGACTGCAGCCACCTG      120
HOE-E6/E7-shTLR3-Exon2      TGTGCATCCTCCCCCACACAAGCGACCGTTAGCACGAAGCCGTCTACCGAGCACCCGAAG      120
                            ************ ****  *    ** ******    *     **  *     **    *

HOE-E6/E7-WT-Exon2          AAGTTGACTCAGGTACCCGAT----   141
HOE-E6/E7-shTLR3-Exon2      CCG----ACCAGGTACCAGTGATCA   141
                              *      ******** *
```

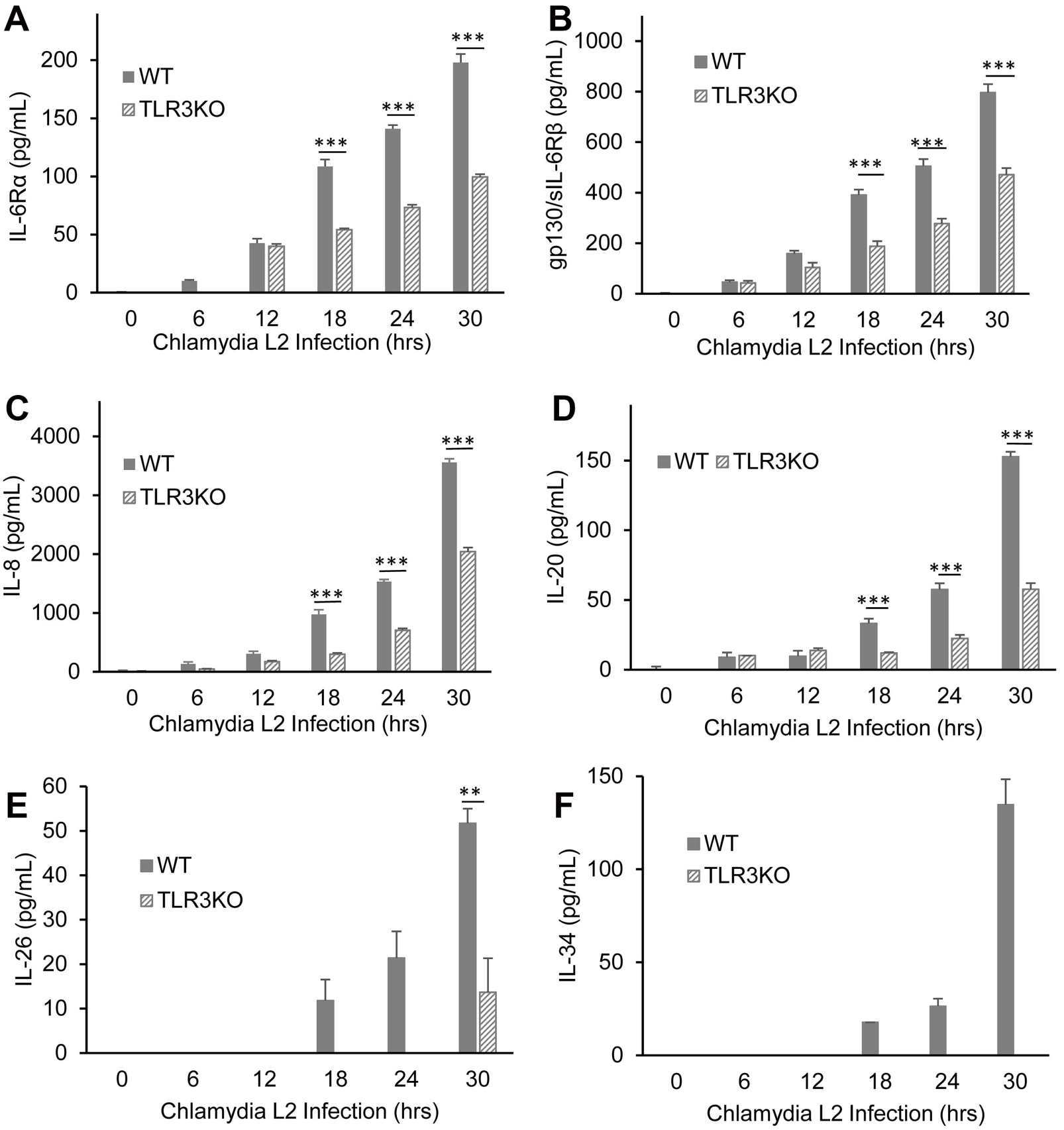

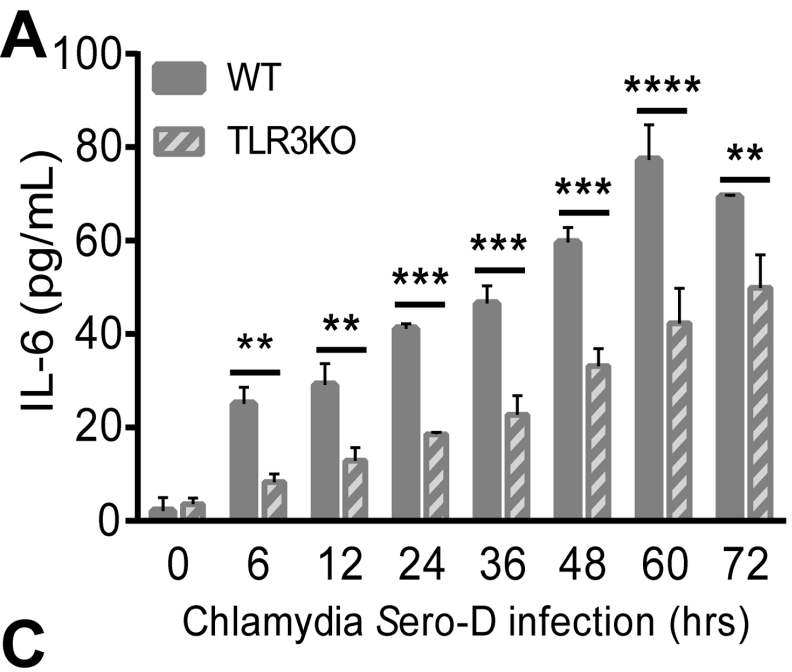

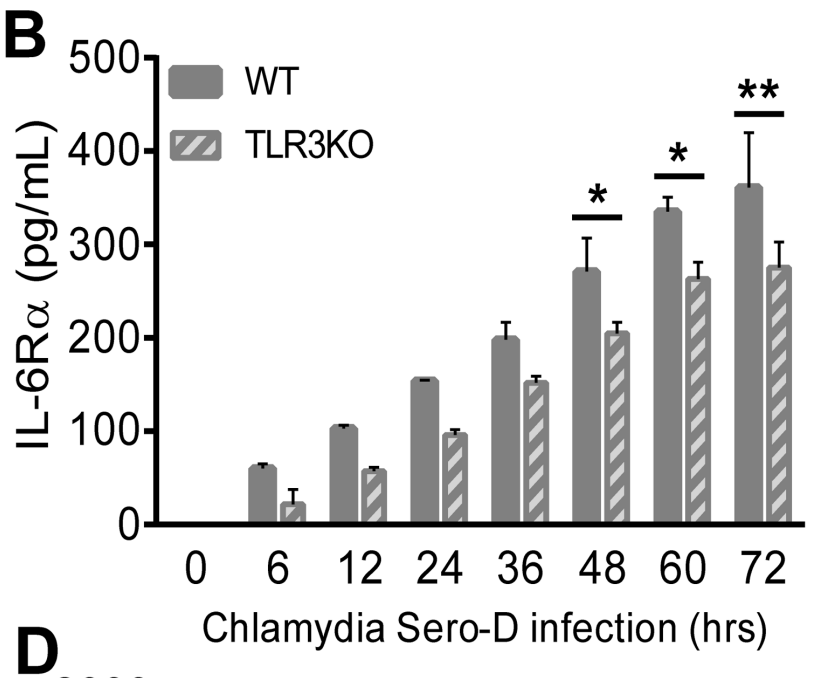

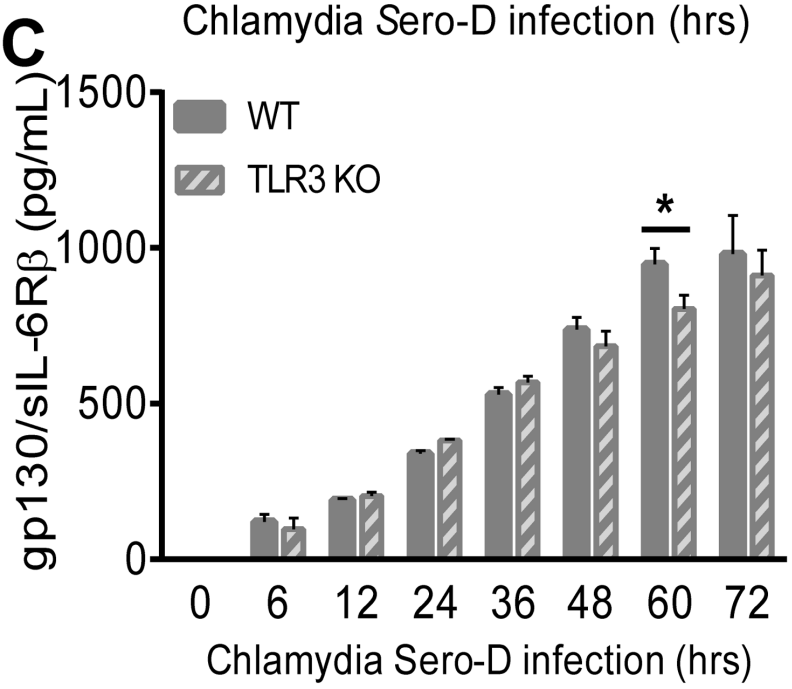

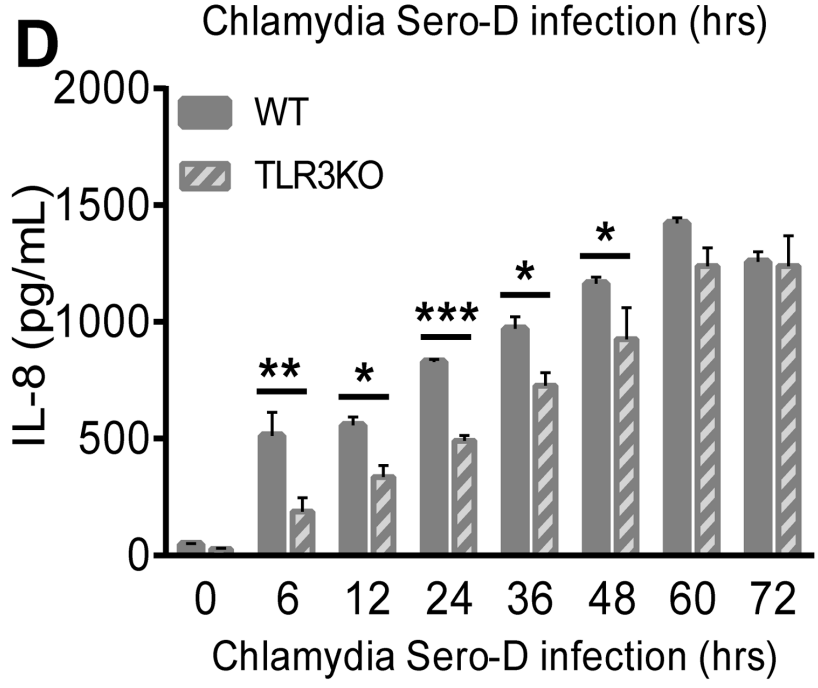

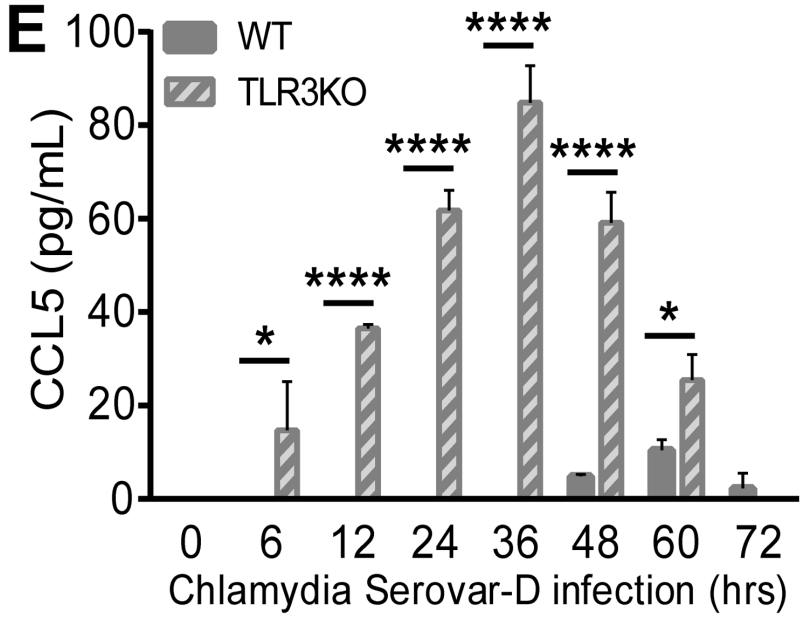

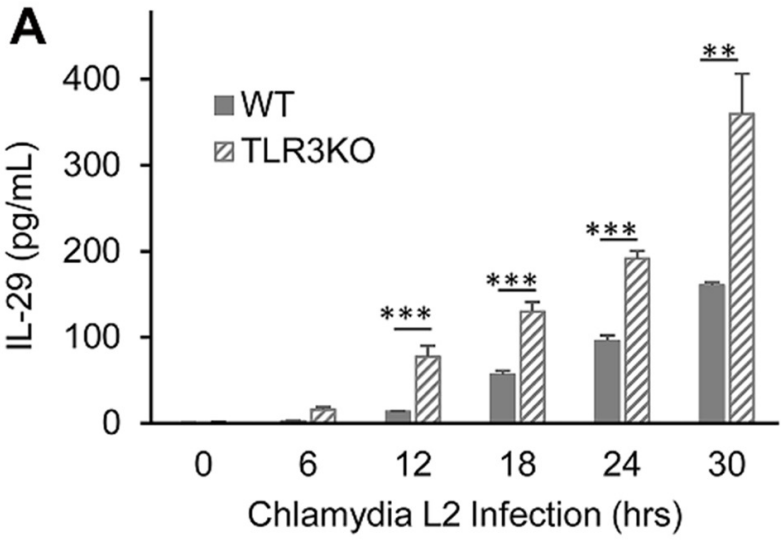

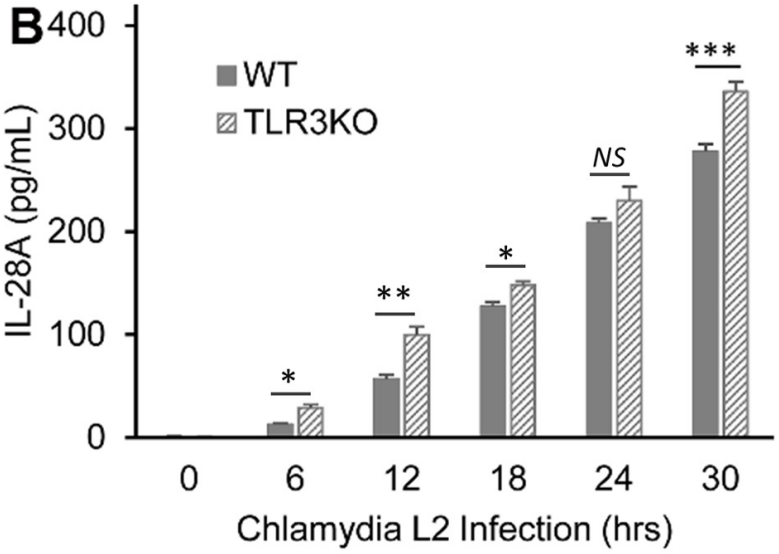

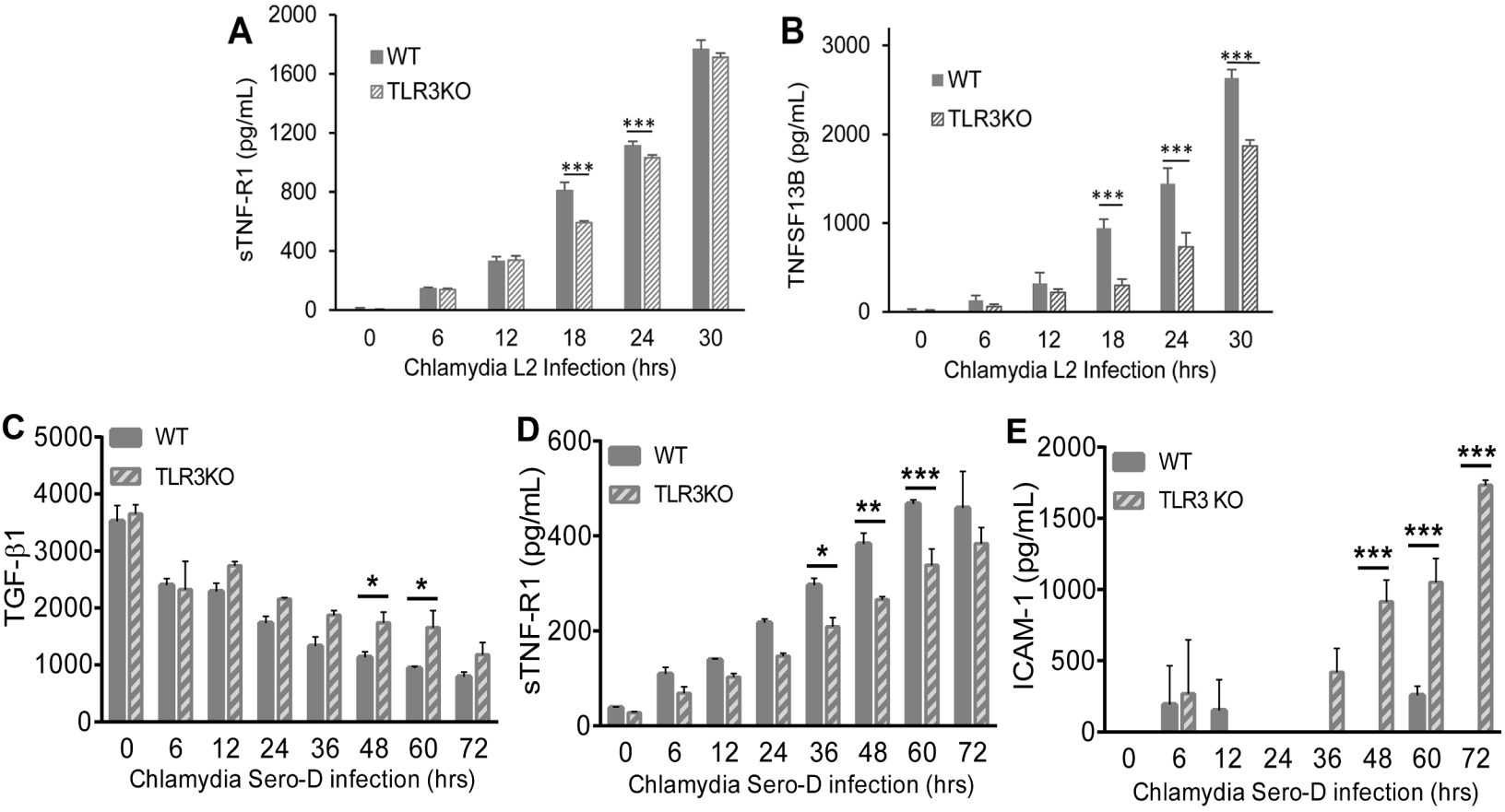

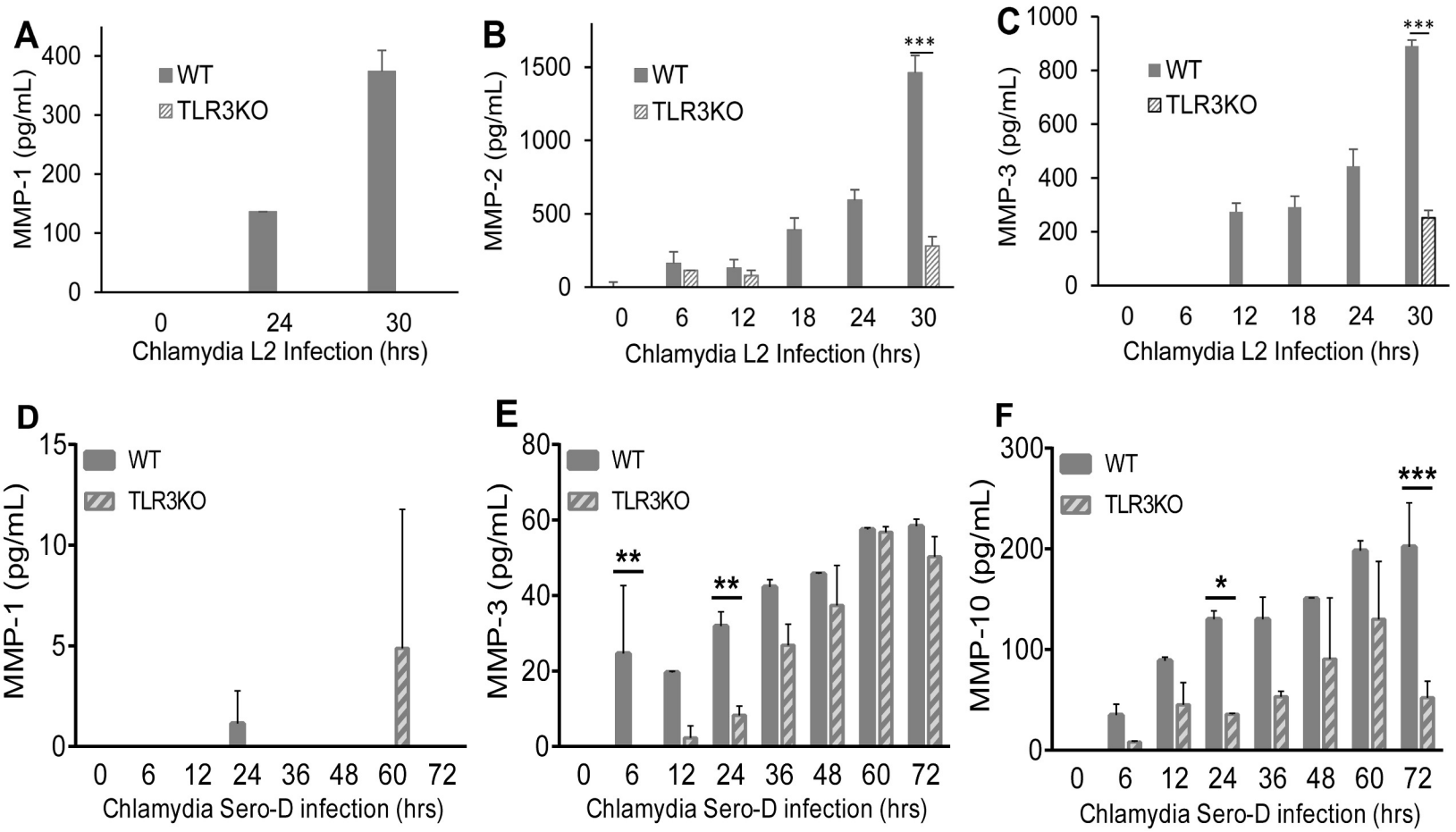

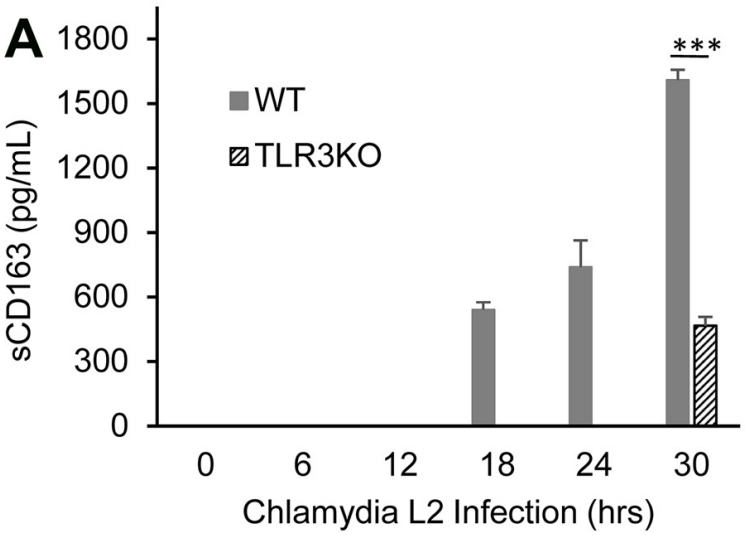

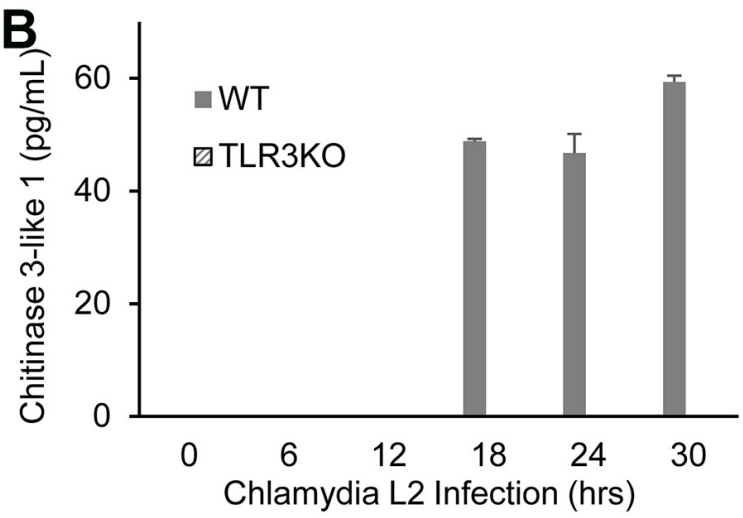

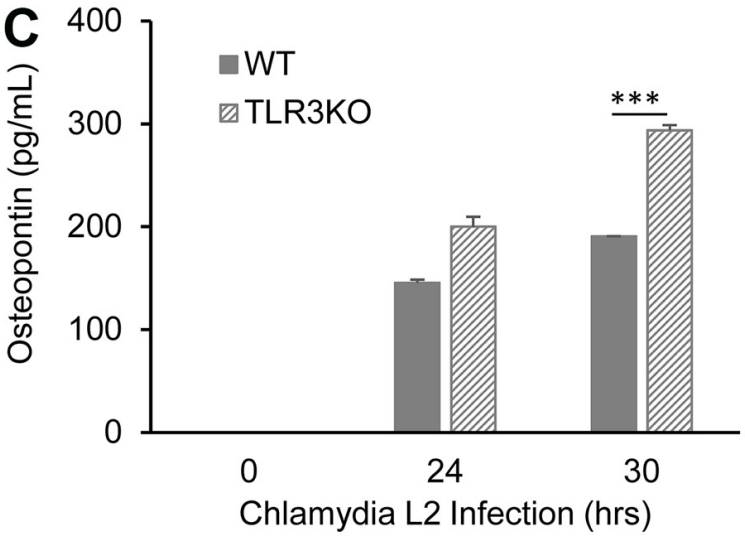

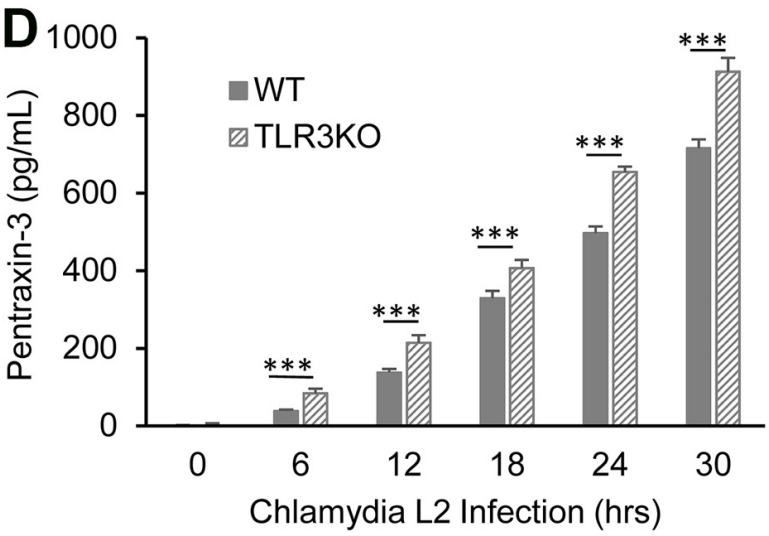

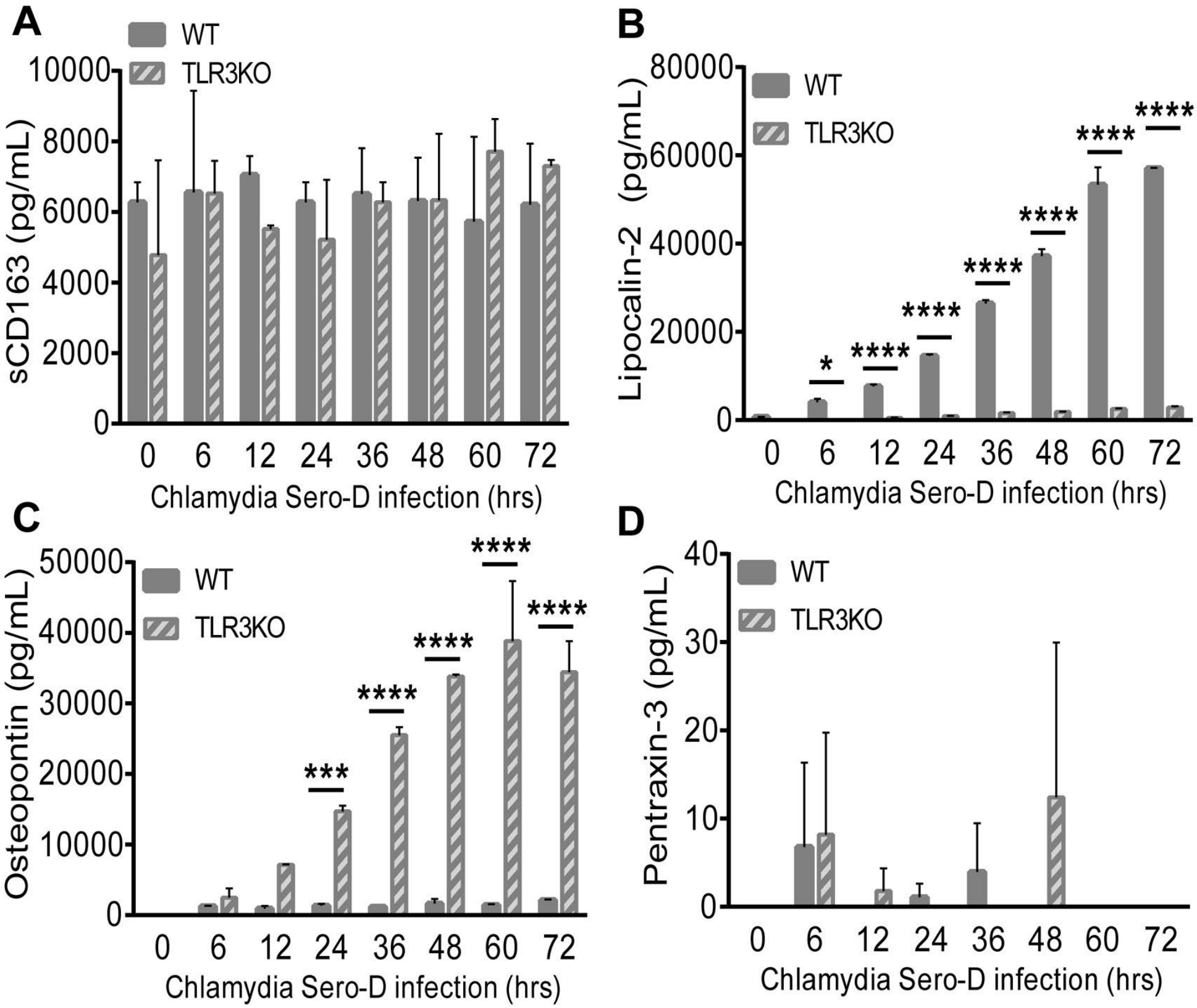
A
WT
TLR3KO
sCD163 (pg/mL)
10000
8000
6000
4000
2000
0
0 6 12 24 36 48 60 72
Chlamydia Sero-D infection (hrs)
B
WT
TLR3KO
Lipocalin-2 (pg/mL)
80000
60000
40000
20000
0
*
****
****
****
****
****
0 6 12 24 36 48 60 72
Chlamydia Sero-D infection (hrs)
C
WT
TLR3KO
Osteopontin (pg/mL)
50000
40000
30000
20000
10000
0
***
****
****
****
****
0 6 12 24 36 48 60 72
Chlamydia Sero-D infection (hrs)
D
WT
TLR3KO
Pentraxin-3 (pg/mL)
40
30
20
10
0
0 6 12 24 36 48 60 72
Chlamydia Sero-D infection (hrs)